

## Responses to Reviewer #2

Thank you to both reviewers for their comments. We have continued to work to clarify the methods and discussion in the manuscript.

The paper presents a nice way to partially isolate the affects of cloud droplet distribution shape on condensation/evaporation by comparing condensation/evaporation rates in a bulk model to a bin model. Statistics are produced for average condensation/evaporation rate binned in terms of distribution properties such as average drop distribution diameter. It is shown that when comparing bulk to bin condensation/evaporation rates, removing the effect of of the distribution shape will generally produce better comparison, expect when evaporation mass fraction is high. While the method is useful more discussion on how to apply the method to improve bulk models is needed.

It is beyond the scope of this paper to determine how to improve the representation of the shape parameter in bulk schemes. The purpose of the paper is to show that the shape parameter is responsible for a large degree of the disagreement between bin and bulk schemes (in terms of condensation/evaporation), and to argue that more work is needed by the community to improve the representation of the shape parameter in models. We are not suggesting that the methods we have used to show that the shape parameter is important should be the same methods used to “fix” bulk schemes. This is now explicitly stated in the conclusions.

### General Comments:

You discuss comparing process rates between bin and bulk in order to improve bulk schemes. So how do you use your analysis to improve bulk schemes? It seems like the parameter space of various values of number concentration, distribution shape, and average cloud droplet size is so large that this study, although useful, would have trouble providing direct improvement to bulk models? Is this correct or is there a good way to use bin models to inform bulk models for condensation/evaporation?

Yes, the reviewer is correct. It would be difficult to use our analysis methods to improve bulk schemes. Though not the topic of the paper, we do feel that searching for robust empirical relationships between the shape parameter (or relative dispersion) of simulated distributions and other cloud properties may be one way to use bin schemes to inform bulk schemes.

Why not use values from the curves from Fig.1 when choosing simulations to run?

This is certainly an approach we could have taken. However, the methods we used to choose values should not impact our results.

Line 95: You state “the lack of a prognosed shape parameter for the cloud droplet size distribution in the bulk scheme is often the primary source of difference between the two schemes.” Why only used a fixed shape parameter in the bulk simulations? Why not diagnose a value? Would diagnosing a value provide better results? How would diagnosing a value change your results? Perhaps diagnosing the shape parameter would leave to better agreement between bulk and bin when evaporation fraction is high.

No good ways to diagnose the cloud droplet shape parameter exist to our knowledge. Some diagnostic equations do exist, but as we discuss in Igel and van den Heever 2017a, most do not seem appropriate for high resolution simulations such as these. We absolutely agree that diagnosing the shape parameter would lead to better agreement – that is essentially one of the points we are trying to make.

Specific Comments:

Abstract

Line 16: I don't agree that the statistics are novel. Maybe replace with "statistically"  
We have made the change.

Manuscript

Line 35: The shape is sometimes fixed as well

We are not sure what the reviewer means by "shape". We state that "a function is assumed to describe the shape of the size distribution ..."

Line 44: Probably can remove discussion on ice as it is irrelevant to the paper  
It has been removed.

Line 64: What parameter are you talking about?

Thank you, the parameter is the shape parameter, and this is now explicitly specified.

Line 107: Remove this line.

We have removed it.

Line 109: PDF is already defined

Thank you. We now just say PDF.

Equations 2 and 3 need periods at the end of the sentence

Thank you, they are now included.

Line 143: What do you mean by this? Do you have a larger range of bins and thus more statistics?

This is a typo. The word should be "wide", not "wider".

Line 146: How deep are the clouds in the simulations? A grid of 3.5km high seems far too shallow.

No cloud top exceeded 2.85km from the surface, and the vast majority of clouds had tops below 2.5km.

Line 196: extra comma

Thank you, it has been removed.

Line 219: Certainly clouds exist between 99-101% RH, and certainly signatures of the drop distribution properties should be between these RHs. Why not just include the analysis?

Also, what percentage of the grid exists between these humidities?

Yes, clouds certainly do exist at RH of 99-101%. In the low aerosol simulations, they are 28-33% of the cloudy points, in the moderate aerosol simulations, they are 42-64% of the cloud points, and in the high aerosol simulations, they are 64-67% of the cloudy points. In the revised paper, we have included all data, and the results are very similar. We have also added a section about the impact of relative humidity on the comparison of the two schemes. This section more clearly demonstrates and explains why RH close to 100% leads to a worse comparison between the two schemes.

Line 234: Extra “)”

Thank you, it has been removed.

Could you possibly get rid of Table 2 and incorporate the standard deviation data into the figures?

Yes. We have removed Table 2 and listed the standard deviation data in the legends of each plot.

Line 249: Evaporation seems to tend towards bulk in Fig. 3A

Agreed. This is now noted.

Line 251: Is the long tail in the condensation or evaporation?

The evaporation.

Line 289: Briefly describe the method used to fit the bin distributions.

We now include such a description. It is reproduced here:

Here we used the maximum-likelihood estimation (MLE) method. For our problem, the log-likelihood function ( $\ln(L)$ ) is defined as

$$\ln L = \frac{1}{N_t} \sum_{i=1}^{15} N_i \ln n(D_i) \quad (4)$$

where  $n(D_i)$  is the value of the gamma PDF (Eq. 1) for  $D_i$  with unknown values of the parameters  $D_n$  and  $\nu$ . The function is normalized by the total cloud droplet concentration  $N_t$  in order to remove  $N_t$  as a free parameter in Eq. 1. As indicated by its name, the MLE method seeks to maximize the log-likelihood function given by Eq. 4. To do so, we used the MATLAB function `fmincon` to find the parameter values that minimized  $-1*L$ .

Line 301: What percentage of the data had best-fit shape parameters less than 1? Did it occur frequently?

For BIN100, BIN400, and BIN1600, it was 4.5%, 5.1%, and 8.6%, respectively. These values are now specified in the manuscript.

Correcting the data seems to make the orange line in Fig. 3C worse. Why?

This is a question that we have spent a considerable amount of time thinking about. We think that the reason may be that differences in the schemes caused by sub-time stepping are more important than the shape parameter differences in this case, but only because the shape parameter used by the BULK simulation was similar to the best-fit shape parameters in the BIN simulation.

Line 351: What does an NRMSE of 2 mean?

There is no particular meaning of an NRMSE of 2, except to say that it is worse than assuming a fit that is independent of the predictor (in this study diameter) and equal to the mean of the data. The NRMSE is defined here as

$$NRMSE = \frac{\sqrt{\sum_{i=1}^{15} (y_i - \hat{y}_i)^2}}{\sqrt{\sum_{i=1}^{15} (y_i - \bar{y})^2}}$$

where  $y_i$  is the simulated probability density of droplet concentration in the  $i$ th bin,  $\hat{y}_i$  is the fitted probability density of droplet concentration in the  $i$ th bin, and  $\bar{y}$  is the average value of all  $y_i$ 's. The sum

runs from 1 to 15 since we have 15 bins containing cloud droplets. Thus if the fitted probability density  $\hat{y}_i$  is equal to  $\bar{y}$  for all  $i$ , the NRMSE is 1.

That said, we did find an error in our calculation of NRMSE. It has been corrected, and as a result, values greater than 1 are now extremely rare. The new cumulative distributions are shown below.

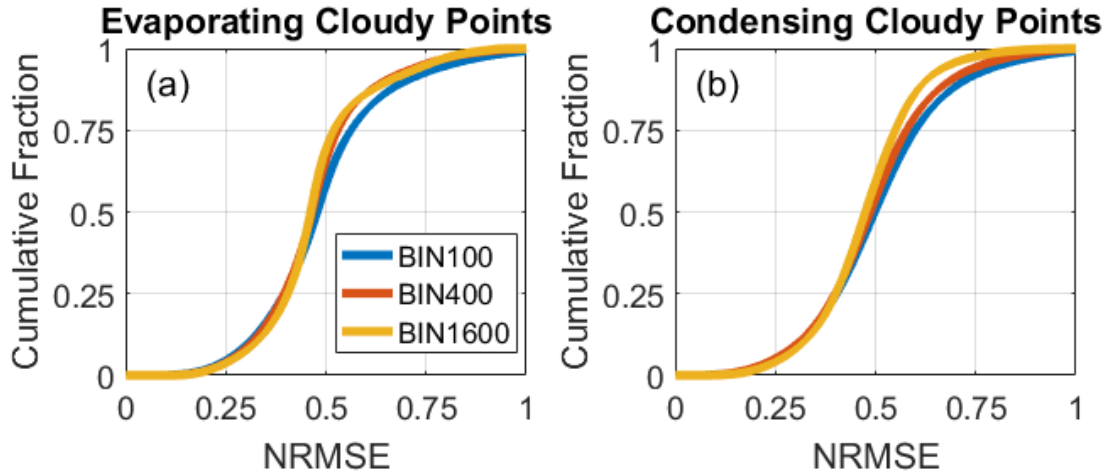
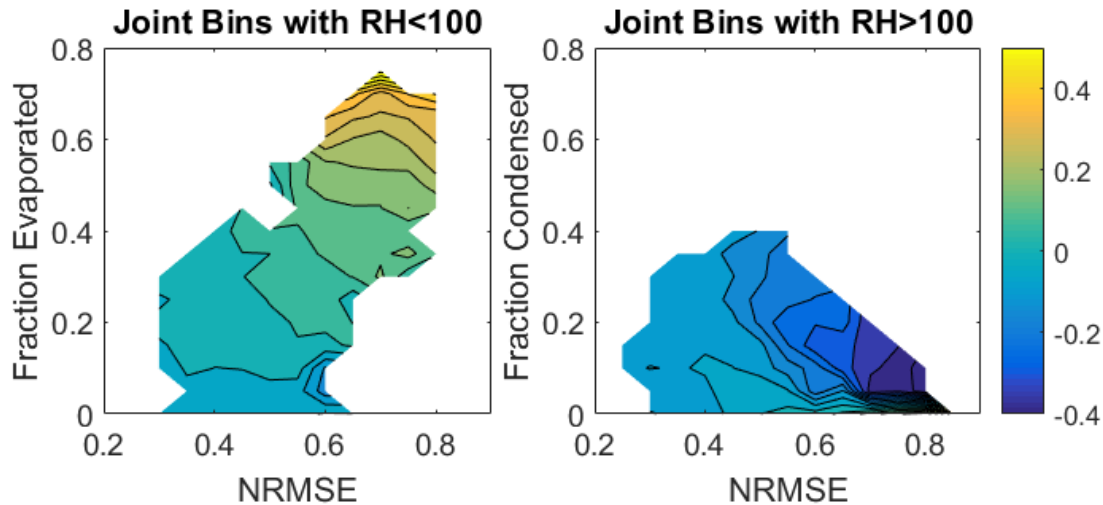


Figure 4. Needs to be explained better in the text. Is it showing that approximately 80% of the cloudy grid points have an NRSME<0.6? Why is 0.6 considered appropriate?

We agree that 0.6 was an arbitrary cutoff value. We have removed this figure and replaced it with a new figure in order to make the same arguments, but in a way that does not require the use of an arbitrary cutoff. Here we show the new Figure and its description.

To explore simultaneously the impact of NRMSE and fractional mass change on the comparison of bin and bulk scheme condensation and evaporation rates, we also calculated the mean NRMSE and fractional mass change of each of the joint  $S$ ,  $N$ , and  $\bar{D}$  bins in addition to the corrected mean  $\ln(\text{ratio})$  for each bin that we have shown previously. In this analysis, we have excluded points with relative humidity between 99.5% and 100.5%. Joint bins with similar mean NRMSE and fractional mass change were grouped together to find a mean of the corrected mean  $\ln(\text{ratios})$ . Joint bins from all simulation pairs were included. The results are shown in Figure 7, again for condensation and evaporation separately, where colors show the mean of the corrected mean  $\ln(\text{ratios})$  as a function of NRMSE and fractional mass change.



Line 395: It can account for some changing drop distribution properties, but not large changes to the shape parameter that may occur when evaporation rates are high. Is this large change in distribution shape during evaporation that the bin model can capture the reason for the difference in Fig. 5A?

Yes, we believe that the bin model's ability to account for the changing distribution during evaporation is the reason for the large differences in Figure 5a (which has been removed since it used an arbitrary cutoff) and the new Figure 7a (shown above).

Maybe move Fig. 4C and 4D to their own figure?

Thanks for the suggestion. With the slightly new development of the discussion, we felt it was better to leave them all as one figure.

Line 443: But what does that high evaporation fraction do to the bin distribution?

We are not entirely sure what the reviewer is asking. Like the reviewer mentioned above, the bin scheme is able to deal with large changes to the size distribution during evaporation in ways that the bulk scheme cannot. In part this is due to the way that the bin scheme uses sub time steps during evaporation and condensation. We believe that it is these differences in the schemes that lead to the dependence on the evaporation fraction.

Conclusion 1: What assumptions were made for the aerosol distribution in the bin model? Was it initially assumed to be a gamma distribution? If so, then it is no surprise that using a gamma distribution would be a good bulk assumption compared with bin.

No, the aerosol distribution was initially lognormal with a median radius of 40nm and a spectral width of 1.8. These details are now included in the description of the simulations. That said, we agree that it may not be surprising that using a gamma distribution is a good assumption. In the revised manuscript, this conclusion has been removed.

Conclusion 2: (Line 468) You didn't show that sub-time stepping is important. Remove this sentence.

The reviewer is correct, we did not directly show that the sub-time stepping is important. However, we did show that the fraction of mass evaporated is important, and we believe that the reason for this

importance relates to the sub-time stepping used by the bin scheme. In the revised conclusions, we do not mention the sub-time stepping.

**Line 473: Specify the conditions that this applies for: Low evaporation fraction, humidities >101%, etc.**

Thank you for the suggestion. We have modified the statement to specify that the conclusion only applies to situations when relative humidity is not near 100%. The other factors, such as low evaporation fraction, seem to be of secondary importance. Earlier the reviewer raised the question about the orange line seeming to be worse after the shape parameter correction. The main reason the shape parameter correction did not have a positive impact was that the shape parameter assumed by the bulk scheme simulation was close to the most common best-fit shape parameter simulated by the bin scheme. In this case, the shape parameter may not have been the most important reason for the two schemes disagreeing, but only because an appropriate shape parameter had been used. When inappropriate values are used (for example the purple and green lines), it is clear that the inappropriate shape parameter was the main cause of the disagreement.

**Remove the talk about radiation and ice in the Appendix**

We would rather include it for the reasons stated before, but it has been removed.

### Responses to Reviewer #3

Thank you to both reviewers for their comments. We have continued to work to clarify the methods and discussion in the manuscript.

#### **Review of study "The role of the Gamma function shape parameter in determining differences between condensation rates in bin and bulk microphysics schemes" authored by A. Igel, and S. van den Heever.**

The rates of condensation and evaporation obtained in simulations with bin and bulk microphysical schemes are compared in simulations of non-precipitating shallow cumulus clouds. It is shown that the difference between the rates is largely because of non-optimum choice of shape parameter in the Gamma distribution used in the bulk-scheme. Corrections in the rates of condensation and evaporation in the bulk -scheme are introduced to get better agreement with those in the bin-scheme.

The topic of the paper is important. The calibration of bulk-parameterization schemes using bin-schemes as benchmark is an important way to improve bulk-schemes and the skill of cloud-resolving models. At the same time I have very serious remarks to the current study. The paper cannot be published in the present way. *I would recommend to discuss the possibility of publication after major revision.*

The comments and remarks are the following.

1. General comment: the paper is written in a very unclear way. It is difficult to follow the conclusions and statements of the authors. The paper contains a lot of complicated discussions, assumptions, and conclusions which are not illustrated either by formulas or by figures. We have worked to clarify the discussion throughout the manuscript. In reading through the reviewer's comments, we see that there were some places where the reviewer did not fully understand our analysis methods. In particular it seems that the reviewer thought that we were implementing the shape parameter correction into the model to run new simulations. This was not the case. This misunderstanding probably led to additional confusion throughout the paper. The analysis methods are described more clearly now, and with a clear understanding of our actual methods, some of the arguments that were confusing before should be clear now.

2. line 73. Is it possible to plot in fig 2 (or in a separate figure) the values of shape parameters that can be derived from the bin scheme used?

Yes. We now show example average shape parameter values from some of the joint bins in BIN400, as well as example values of  $\overline{f_{NU,BIN}}$ . Here is the new figure 2:

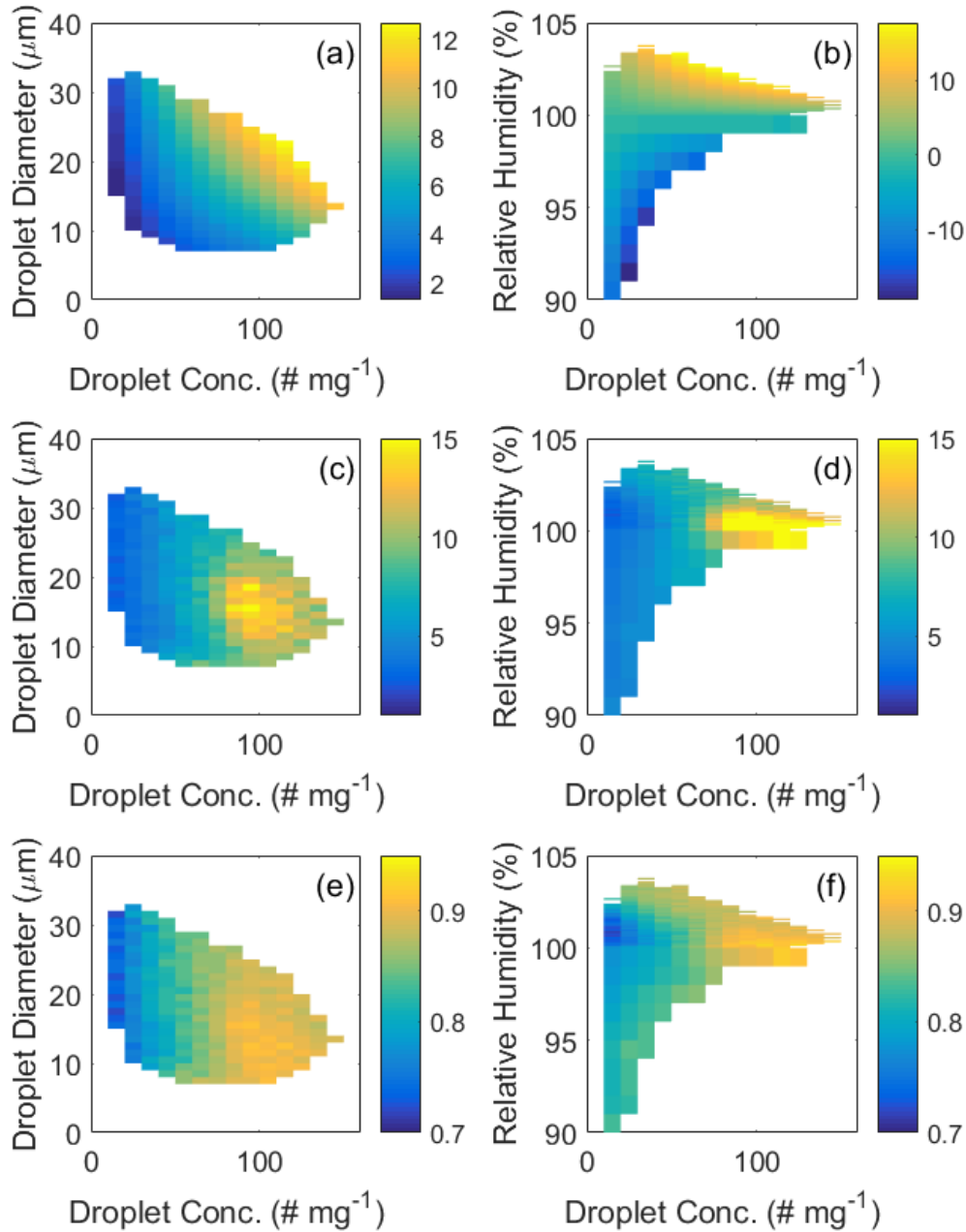


Figure 2. (a, b) Example average condensation and evaporation rates ( $\text{mg kg}^{-1} \text{s}^{-1}$ ), (c, d) example average shape parameters, and (e, f) example average values of  $f_{NU,BIN}$  in joint bins from BIN400. (a, c, e) show average values of the two quantities for all joint bins from BIN400 with  $S$  between 1.011-1.012 and (b, d, f) show averages for all joint bins from BIN400 with  $\bar{D}$  between 19 and 20  $\mu\text{m}$ .

3. line 114. Does the expression (2) mean that supersaturation is assumed constant during one time step? I suppose that it is not a good approach, because drop growth and the changes of  $S$  are actually described by the same equation. Namely, when droplet grow they immediately decrease  $S$ . It is just the mass conservation law.

Supersaturation is not assumed constant during a time step. The RAMS' representation of condensation is actually relatively sophisticated compared to most bulk schemes in that simultaneously accounts for both vapor and heat diffusion to/from hydrometeors. A complete description of the condensation/evaporation is beyond the scope of this paper. We only want to point out the most basic differences between bulk and bin schemes. Based on this comment and many of those that follow, it seems that in our effort to be complete in writing down the condensation equations from the two schemes, we have created more confusion than is necessary. In the revised manuscript, we only indicate the how the condensation rate is proportional to  $S$  and the droplet distribution properties without discussing the details of the implementation except where necessary.

4. Most bulk schemes use saturation adjustment, which likely decrease the accuracy of those bulk schemes as compared to that used in RAMS. To what extent the values of corrected factors (eq. (4)) are suitable for other bulk schemes?

The results of this study should not be applied to bulk schemes that use saturation adjustment. This is now explicitly stated in the conclusions.

5. line 116. 1) Eqs (2) and (3) contain very strange notations:  $r$  is not the radius (typical notation), but mass mixing ratio. 2) from the notations it is not seen that  $r_c$  in (2) is cloud water content (CWC), and in Eq. (3)  $r_c$  is mass content of droplets belonging to the  $i$ -th bin in the bin scheme. The utilization of the same notations to different quantities leads to confusion, and leads to the necessity of long explanations in the text. I would recommend to use bin indexes in case the bin scheme is discussed.

We agree that  $r$  is often radius, but it is also usually the symbol used for mixing ratio (e.g. the AMS Glossary entry for mixing ratio). In the revised equations, only  $\partial r_c / \partial t$  appears, and the definition of this term is explicitly stated.

6. line 116. Most bulk schemes use saturation adjustment, which likely decrease the accuracy of those bulk schemes as compared to that used in RAMS. To what extent the results about the choice of the shape parameter (or corrections implemented in eq. 4) are suitable for other bulk schemes?

Schemes that use saturation adjustment should not be at all sensitive to the choice of shape parameter, and the results of this study will not be applicable to those schemes. This is now made clear in the conclusions.

7. line 125. Table 1 present notations. The table does not present explanations. I suppose the expressions for condensational/evaporation growth should be presented clearer.

Yes, we only intended Table 1 to give definitions of the symbols. We have eliminated Table 1 given that we have substantially simplified Eqs. 2 and 3.

8. line 133. What is time step used in BULK in Eq. (2)? The characteristic time scale of the change of  $S$  is drop relaxation time during which  $|S-1|$  falls trice. Time step should be smaller than the drop relaxation time. Otherwise utilization of the Eulerian integration scheme can lead to  $RH < 100\%$  in case of condensation. (This is the reason of the utilization of substeps in the bin-scheme).

It is the full model time step (1s). Notice in the previous version of the manuscript that Eq. 2 uses  $S^{t+\Delta t}$ . This makes the equation implicit. Without going into the details, Eq. 2 is a simplified and incomplete version of the actual equations used in the condensation scheme. The methods

used to solve this implicit equation are such that if  $RH > 100\%$ , it will still be  $\geq 100\%$  at the end of the time step. See Walko et al. (2000) for full details.

9. line 158. It is not clear how do you use the approach to calculate  $S$  in the bulk scheme using the approach used in the bin scheme. Do you mean that you used analytic solution for  $S$ ? How did you calculate coefficients in the equations supersaturations  $S$  and  $S_i$ , which (i.e. coefficients) include size distributions? If you know supersaturation integral, why do you not use the bin-emulating procedure of recalculation of drop masses in each "bulk" bin?

We have made this clearer. We are only referring to the calculation of the saturation ratio at the beginning of the microphysics routines. We wanted to make sure that both schemes would diagnosis the same value of the saturation ratio from water vapor mixing ratio and temperature. This was originally not the case. The bulk scheme originally used an empirical formula, and the bin scheme used a formula based on the Clausius-Clapeyron equation.

10. line 172. The shape parameters may change with height because the shape of DSD changes. Sometimes the shape parameter should be changed together with other parameters of Gamma distribution.

Some bulk microphysics schemes do have methods for diagnosing the cloud droplet shape parameter. Our scheme does not. A constant value in time and space must be used.

11. line 186. There is no  $v$  in eq (3)

Yes, that is correct.

12. line 193. Correct typo.

Thank you, it has been corrected.

13. Line 207 It is not clear how calibration can be performed when the bulk and the bin-schemes produce different droplet concentrations (because of different reasons including differences in aerosol concentrations). If droplet concentrations are different, it means that the DSD shapes in BULK and BIN should be different just because the DSD shape depends on the droplet concentration. It seems to me that it would be better to choose aerosol concentration in BULK in such a way to get similar droplet concentrations in BULK and BIN.

It is because of these concerns that we are binning all of the output by number concentration (and mean diameter and saturation ratio). This way, we only compare cloudy points in from the bulk simulations with cloudy points from the bin simulations that have very similar number concentrations.

14. line 219. Supersaturation of 1% is quite large value. It is not clear why grid points with such and lower values were excluded from the analysis.

These points are no longer excluded from the initial analysis. We also have included a new section where we more clearly show how our results depend on relative humidity and how the initial analysis changes if we exclude points with  $RH$  of 99.5-100.5% (rather than 99-101% as we did in the previous version of the manuscript).

15. line 227. Fig. 2 is not clear. What is plotted in the figure? How were these figures obtained? Among many questions concerning this figure: why the condensation or evaporation rates are positive at any  $RH$ . Are these diagrams obtained by averaging over cloud volume? Over cloud life time?

Thank you for catching this mistake. This was the wrong plot. It was showing shape parameter, not condensation rate. The correct figure is now included in the manuscript.

16. line 238 In fig 3 "original", but not ORIG.

Thank you. In the revised manuscript, this sentence has been removed.

17. line 317. What are the values of the ratio  $f_{nu, bin}/f_{nu, bulk}$ ? Are these bulk are time and spatial averaged?

At your suggestion, we have included in Figure 2 examples of  $\overline{f_{NU, BIN}}$  from BIN400 (see comment #2). These are average values of all cloudy points that fall in each joint bin, regardless of where they occurred in space or time. The values of  $f_{nu, bin}/f_{nu, bulk}$  will of course depend on which bulk simulation is being compared to each bin simulation. Specifically,  $f_{NU, BULK} = 0.69, 0.81, \text{ and } 0.88$  for NU2, NU4, and NU7, respectively. These values are now specified in the manuscript.

18. If  $f_{nu, bin}/f_{nu, bulk}$  are calculated for each phase space bin, do you calculate a lookup tables to use in bulk simulations? How would these values depend on the stage of cloud evolution and on cloud parameters (cloud top height). How would these values depend on aerosol concentration?

Can you present tables of these values? The application of formula (4) should be described clearer with examples of size distributions, the fields of CWC, fields of concentration, mean volume radius, etc.

We did not explain clearly what we are doing. We are not rerunning any bulk simulations with information about  $f_{nu, bin}/f_{nu, bulk}$ , so there is no need to create look-up tables. We are only taking the outputted condensation/evaporation rates from the bulk simulations, adjusting their values using  $f_{nu, bin}/f_{nu, bulk}$ , and then re-comparing to the bin condensation/evaporation rates. Another way to say this is that we are taking our original  $\ln(\text{ratios})$  (which is different for every joint bin and simulation pair) and multiplying them by  $f_{nu, bin}/f_{nu, bulk}$  (which is also different for every joint bin and every simulation pair) and looking at how the histograms of these adjusted  $\ln(\text{ratios})$  change.

19. line 338. Please provide DSD in bulk and DSD in bin before and after correction.

The DSDs themselves do not change. Hopefully this makes sense given the better explanation of our methods.

20. Please present comparison of fields of CWC (and concentrations) in bin and in bulk scheme before and after corrections. Only such comparison can say whether the correction introduced in (4) led to improvement of the bulk scheme.

CWC and droplet concentrations do not change as a result of the correction since we are not running new simulations.

21. line 433. I suppose that it is necessary to compare DSD in bin and bulk schemes. Otherwise it is impossible to understand what were the changes in the DSD in the bulk scheme as a result of correction expressed by eq. (4).

This comment seems to be related to our inadequate description of our methods. There were no changes to the DSD as a result of (4). Hopefully this is clear now.

22. lines 440-444. The discussion is not clear. The changes in the shape (and amplitude) of DSD can be recalculated into the changes condensation/evaporation rates. So, these changes are closely related. Again, what were the changes in DSD predicted by bulk-scheme after correction expressed by (4)?

This section has been substantially revised. As mentioned above, the bulk scheme simulations have not been rerun, so there are no changes to the DSD to discuss.

23. lines 462-472. The conclusions should be formulated better. First, which results of the authors justify that the Gamma distribution is a good assumption of the DSD? I did not find such justifications in the paper.

This conclusion has been removed. We made this statement based on the fact that the NRMSE values were reasonably low, and that by assuming that the BIN simulated gamma DSD's we could get good agreement in terms of condensation/evaporation rates with the BULK simulations.

Second, immediately, the authors state that the exact knowledge of the shape is not necessary. We meant that having the detailed binned distribution information may not be necessary – an assumption of a gamma PDF may be sufficient if the proper shape parameter is known.

Third, immediately after these conclusions, the authors conclude that the shape parameter is responsible for agreement/disagreement with the bin -scheme results. All these statements seem contradict each other. The text should be shortened and rewritten clearer.

Thank you. The conclusions have been modified to make these points clearer.

24. line 474. Despite the statement that the shape parameter is the main factor that allows to perform calibration, the procedure expressed by (4) does not correct the shape parameter, but just adjusts condensation/evaporation rates. What is the advantage of such approach vs the correction of the shape parameter itself.

The reviewer is correct in that (4) only adjusts the condensation/evaporation rates based on our knowledge of how the best-fit shape parameters in the bin simulations differ from the assumed shape parameters in the bulk simulations. This is a procedure that we have used in order to demonstrate that the shape parameter is important for the different condensation and evaporation rates predicted by the two schemes. In an actual simulation, we would not want to use such a correction, but would instead want to have the correct value of the shape parameter at every cloudy grid point.

It seems that this factor should depend on aerosol concentration

The distribution of best-fit shape parameters (and therefore also correction factors) that arise in the bin simulations does depend on aerosol concentration. Below is a figure from Igel and van den Heever 2017a showing the distributions of best-fit shape parameters from these simulations.

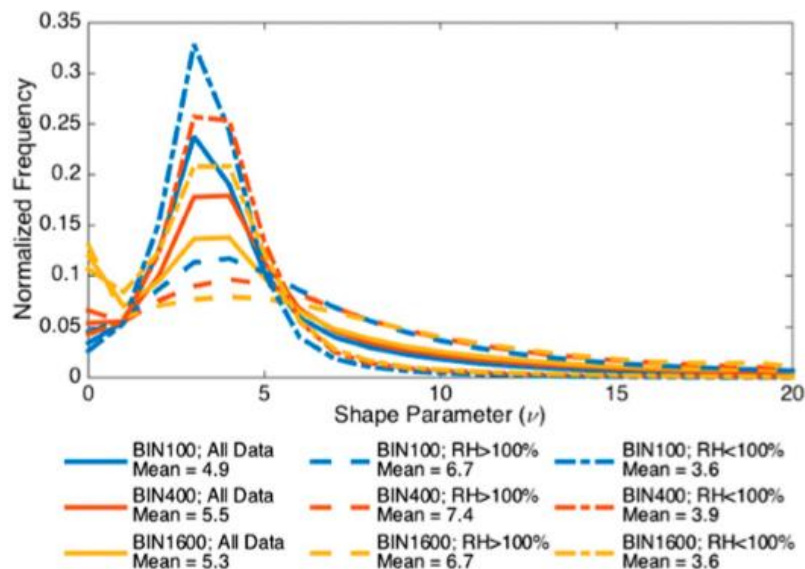


FIG. 5. Frequency distributions of the best-fit shape parameters. Frequency distributions from BIN100, BIN400, and BIN1600 are shown in blue, red, and yellow, respectively. The different line styles show the distribution using all data (solid), data from supersaturated regions (dashed), and data from subsaturated regions (dotted-dashed).

25. Line 485. The conclusions should be formulated clearer. What the authors propose to do with their bulk-scheme: to multiply the condensation/evaporation rates by some factor? Will this factor be tabulated according to certain conditions, cloud stage evolution, etc.?

We are suggesting that more work needs to be done to appropriately diagnose or predict the shape parameter in bulk microphysics schemes in order to improve their ability to simulate clouds. The best way to diagnose or predict the shape parameter is not addressed by the paper. We have made this clearer in the revised manuscript.

### **Relevant Manuscript Changes:**

1. Changes throughout the manuscript to clarify the methods, discussion, and conclusions.
2. Tables 1 and 2 have been removed. Table 1 was removed after Eqs. 2 and 3 were simplified and used far fewer symbols, and Table 2 was removed at the suggestion of Reviewer #2.
3. Figure 2 has been corrected, and additional panels have been added to show shape parameter and  $f_{\text{NU}}$ .
4. Figure 3 has been modified to include the standard deviation data in the legends (instead of in Table 2) and no longer excludes data based on relative humidity.
5. Figures 4 and 5 are new. Figure 4 addresses the dependence of the agreement on relative humidity. Figure 5 repeats the analysis in Figure 3 (Figure 5 is similar to the original Figure 3). New discussion accompanies both figures.
6. Figure 7 replaces the previous Figure 5 and more clearly shows the dependence of the agreement on NRMSE and fractional mass change. Most of the discussion related to these figures has been rewritten.

1 The Role of the Gamma Function Shape Parameter in Determining  
2 Differences between Condensation Rates in Bin and Bulk Microphysics  
3 Schemes

4  
5 Adele L. Igel<sup>1,2\*</sup> and Susan C. van den Heever<sup>1</sup>

6 <sup>1</sup>Department of Atmospheric Science

7 Colorado State University

8 Fort Collins, Colorado

9 <sup>2</sup>Department of Land, Air and Water Resources

10 University of California, Davis

11 Davis, California

12  
13 ~~<sup>†</sup>Corresponding~~ \*Corresponding author:

14 ~~1371 Campus Delivery, Fort Collins, CO 80528~~ 1 Shields Avenue, Davis, CA 95616

15 ~~adele.igel@colostate.edu~~ igel@ucdavis.edu

16

17 **Abstract.** The condensation and evaporation rates predicted by bin and bulk microphysics  
18 schemes in the same model framework are compared in a ~~novel~~statistical way using simulations  
19 of non-precipitating shallow cumulus clouds. Despite other fundamental disparities between the  
20 bin and bulk condensation parameterizations, the differences in condensation rates are  
21 predominantly explained by accounting for the width of the cloud droplet size distributions  
22 simulated by the bin scheme. ~~While~~ ~~the~~ bin scheme does not always predict a cloud droplet size  
23 distribution that is well represented by a gamma distribution function (which is assumed by bulk  
24 schemes); ~~however~~, this fact ~~does not appear to be important~~appears to be of secondary  
25 importance for explaining why the two scheme ~~types~~ predict different condensation and  
26 evaporation rates. The width of the cloud droplet size is not well constrained by observations and  
27 thus it is difficult to know how to appropriately specify it in bulk microphysics schemes.  
28 However, this study shows that enhancing our observations of this width and its behavior in  
29 clouds is important for accurately predicting condensation and evaporation rates.

## 30 1. Introduction

31

32 Bin and bulk microphysics schemes are both popular approaches for parameterizing subgrid-  
33 scale cloud processes as evidenced by the large number of schemes that have been developed.  
34 Tables 2 and 3 in Khain et al. (2015) summarize the characteristics of dozens of microphysics  
35 schemes, and discuss in detail the basic principles of the two basic types of schemes. Briefly, in  
36 double-moment bulk schemes, the mass mixing ratio and total number mixing ratio for  
37 predefined hydrometeor species are predicted, and a function is assumed to describe the shape of  
38 the size distribution of each species. In contrast, bin schemes do not assume a size distribution  
39 function, but instead, the distribution is broken into discrete size bins, and the mass mixing ratio  
40 is predicted for each bin. Usually the size of each bin is fixed, in which case the number  
41 concentration is also known for each bin.

42

43 Bin schemes, particularly those for the liquid-phase, are generally thought to describe cloud  
44 processes more realistically and accurately than bulk schemes, and thus they are often used as the  
45 benchmark simulation when comparing simulations with different microphysics schemes (e.g.  
46 Beheng, 1994; Seifert and Beheng, 2001; Morrison and Grabowski, 2007; Milbrandt and Yau,  
47 2005; Milbrandt and McTaggart-Cowan, 2010; Kumjian et al., 2012). ~~For the ice phase, bin~~  
48 ~~schemes are subject to many of the same issues as bulk schemes, such as the use of predefined~~  
49 ~~ice habits (which may not always appropriately describe real-world ice) and the conversion~~  
50 ~~between ice types (the real atmosphere does not have strict categories for ice), rendering them~~  
51 ~~not necessarily more accurate (Khain et al. 2015). Regardless, b~~Bin schemes are much more  
52 computationally expensive since many additional variables need to be predicted. As a result, bin

53 schemes are used less frequently. It is of interest then to see how well bulk and the more accurate  
54 liquid-phase bin microphysics schemes compare in terms of predicted process rates, and to assess  
55 how much predictive value is added by using a bin instead of a bulk microphysics scheme.  
56 Furthermore, comparison of process rates in bin and bulk schemes could help to identify ways in  
57 which to improve bulk schemes.

58

59 One of the primary drawbacks of double-moment bulk schemes that assume probability  
60 distribution functions (PDFs) is that many microphysical processes are dependent on the  
61 distribution parameters that must be either fixed or diagnosed. In the case of a gamma PDF  
62 which is typically used in bulk schemes, this parameter is the shape parameter. The gamma size  
63 distribution ( $n$ ) is expressed as

$$64 \quad n(D) = \frac{N_t}{D_n^v \Gamma(v)} D^{v-1} e^{-D/D_n} \quad (1)$$

65 where  $v$  is the shape parameter,  $N_t$  is the total number mixing ratio,  $D$  is the diameter, and  
66  $D_n$  is called the characteristic diameter. All symbols are defined in Table 1 for reference.  
67 Much is still to be learned regarding what the most appropriate value of the shape parameter is  
68 and how it might depend on cloud microphysical properties.

69

70 Figure 1 shows previously proposed relationships between the cloud droplet number  
71 concentration and the shape parameter (Grabowski, 1998; Rotstayn and Liu, 2003; Morrison and  
72 Grabowski, 2007; hereinafter G98, RL03, and MG07, respectively) along with values of the  
73 shape parameter reported in the literature and summarized by Miles et al. (2000) for several  
74 different cloud types. The figure shows a wide range of possible values of the shape parameter  
75 based on observations. The lowest reported value is 0.7 and the highest is 44.6, though this

76 highest point is clearly an outlier. Furthermore, there is no apparent relationship with the cloud  
77 droplet concentration in the data set as a whole, and both increases and decreases of the shape  
78 parameter are found with increasing droplet concentration among individual groupings. There is  
79 also no clear dependence of the shape parameter on cloud type. Figure 1 additionally shows that  
80 two of the proposed functions relating these two quantities are similar (RL03 and MG07), but  
81 that the third function (G98) exhibits an opposite trend compared with these first two.

82

83 Furthermore, using appropriate values of the shape parameter may be necessary to accurately  
84 model cloud characteristics and responses to increased aerosol concentrations. Morrison and  
85 Grabowski (2007) found that switching from the MG07 to the G98  $N$ - $v$  relationships in Figure 1  
86 led to a 25% increase in cloud water path in polluted stratocumulus clouds. This example shows  
87 that inappropriately specifying the shape parameter could have implications for the accurate  
88 simulation of not only basic cloud and radiation properties but also for the proper understanding  
89 of cloud-aerosol interactions. However, it is apparent from Figure 1 that *large uncertainties still*  
90 *exist regarding the behavior of the shape parameter and how it should be represented in models.*  
91 The goal of this study is to compare the condensation and evaporation rates predicted by bin and  
92 bulk microphysics schemes in cloud-resolving simulations run using the same dynamical and  
93 modeling framework and to assess what the biggest sources of discrepancies are. The focus is on  
94 condensation and evaporation since these processes occur in all clouds and are fundamental for  
95 all hydrometeor species. It will be shown that in spite of other basic differences between the  
96 particular bulk and bin microphysics schemes examined here, the lack of a prognosed shape  
97 parameter for the cloud droplet size distribution in the bulk scheme is often the primary source of

98 differences between the two schemes. Thus, an improved understanding of the shape parameter  
 99 is necessary from observations and models.

100

## 101 2. Condensation/Evaporation Rate Formulations

102 The Regional Atmospheric Modeling System (RAMS) is used in this study. It contains a double-  
 103 moment bulk microphysics scheme (BULK) (Saleeby et al., 2004) and the Hebrew University  
 104 spectral bin model (BIN) (Khain et al., 2004). The Hebrew University spectral bin model is  
 105 newly implemented in RAMS. Details about the implementation can be found in Appendix A.

106

107 In the BULK microphysics scheme, ~~condensation/evaporation is treated with a bulk approach.~~  
 108 ~~C<sub>cloud</sub> droplet size distributions are assumed to conform to a gamma probability distribution~~  
 109 ~~function (PDF) PDF given by Eq. (1). The condensation/evaporation scheme is described in detail~~  
 110 ~~in Walko et al. (2000), and the amount of liquid water condensed in a time step is given by their~~  
 111 ~~Eq. 6. Here, a slightly rearranged and simplified version of this equation is presented in order to~~  
 112 ~~highlight the similarities to the BIN condensation/evaporation equation shown below. only the~~  
 113 ~~important relationships to the cloud droplet distribution properties are shown.~~ Specifically, the  
 114 BULK condensation/evaporation rate ( $\partial r_c / \partial t$ ; time rate of change of the mass mixing ratio of  
 115 cloud droplets) is proportional to  $N_t$ ,  $\bar{D}$  (mass mean diameter),  $v$ , and  $S$  in the following  
 116 way: equation is written as

$$117 \frac{\partial r_c}{\partial t} \propto (S - 1) r_e^{t+\Delta t} = r_e^* + 2\pi \left[ N \bar{D} v \left( \frac{\Gamma(v)}{\Gamma(v+3)} \right)^{1/3} f_{v,BULK} \right] N_t \bar{D} v \left( \frac{\Gamma(v)}{\Gamma(v+3)} \right)^{1/3} G_{BULK}(S^{t+\Delta t} -$$

118  $1) \Delta t.$  (2)

119 The BULK scheme does not use a saturation adjustment scheme for cloud water like many other  
 120 bulk microphysics schemes do. Also, while not obvious here, the BULK scheme

121 condensation/evaporation is implemented in such a way that evaporation cannot result in  
122 supersaturation, and likewise condensation cannot deplete the water vapor so much that the air is  
123 subsaturated at the end of the time step.

124  
125 In contrast, the equation for the condensation/evaporation rate in the BIN is given by proportional  
126 to  $S$ , and the number concentration  $N$  and diameter  $D$  in each bin in the following way:

$$127 \quad \frac{\partial r_c}{\partial t} r_c^{t+\Delta t} \propto (S - 1) \sum N_i D_i = r_c^* + 2\pi \left( \sum N_i D_i f_{v,i,BIN} \right) G_{BIN} \int_0^{\Delta t} (S - 1) dt. \quad (3)$$

128 As we would expect in a bin scheme, the condensation rate is proportional to the droplet  
129 properties in each bin rather than on the average droplet diameter and total number  
130 concentration. In the bin scheme, many small sub-time steps are taken during  
131 condensation/evaporation and the values of  $S$ ,  $N_i$ , and  $D_i$  are updated after each. Semi-analytical  
132 equations are used to solve for the time integral of supersaturation that appears at the end of Eq.  
133 3 (Khain and Sednev, 1996). In both equations,  $r_c$  is the cloud mass mixing ratio,  $f_v$  is the  
134 ventilation coefficient,  $G$  is a term that accounts for latent heating, vapor diffusion and heat  
135 diffusion,  $S$  is the saturation ratio, and  $t$  is time. The saturation ratio is defined as the ratio of the  
136 water vapor partial pressure to the saturated water vapor partial pressure. More details are given  
137 in Table 1.

138  
139 Although both equations have the same basic form, there are two primary differences in how  
140 these equations are formulated:

- 141 • In the BIN, as is required by the model structure, the condensation rate is calculated for  
142 each bin of the distribution, and these rates are then summed over all bins, as opposed to  
143 the integration of the gamma distribution that is done in the BULK scheme.

144 • ~~The time step integration is performed semi-analytically in the BIN with multiple sub-~~  
145 ~~time steps rather than implicitly in the BULK scheme.~~

146 ~~These differences between the bin and bulk schemes will be taken into consideration in this~~  
147 ~~analysis in order to understand why the two schemes produce different condensation rates.~~  
148

### 149 3. Simulations

150 In order to investigate the difference in condensation rates predicted by the two microphysics  
151 schemes, simulations of *non-precipitating* shallow cumulus clouds over land were performed.

152 This cloud type was chosen in order to minimize the indirect impacts of precipitation processes.

153 Furthermore, the daytime heating and evolution of the boundary layer results in a wider range of

154 thermodynamic conditions than would occur in simulations of maritime clouds. ~~The wider range~~

155 ~~of thermodynamic conditions make the conclusions of this study more robust.~~ The simulations

156 were the same as those described in Igel ~~et al.~~ and van den Heever ~~2016a~~2017a-b. They were run

157 with RAMS and employed 50m horizontal spacing and 25m vertical spacing over a grid that is

158 12.8 x 12.8 x 3.5 km in size. Such fine spacing was used in order to well resolve the cumulus

159 clouds and their microphysical structure. The simulations were run for 9.5 hours using a 1s time

160 step. Clouds appeared after about 4.5 hours. The simplified profiles of potential temperature,

161 horizontal wind speed, and water vapor mixing ratio based on an Atmospheric Radiation

162 Measurement (ARM) Southern Great Plains (SGP) sounding from 6 July 1997 at 1130 UTC (630

163 LST) presented in Zhu and Albrecht (2003) (see their Fig. 3) were used to initialize the model

164 homogeneously in the horizontal direction. Random temperature and moisture perturbations

165 were applied to the lowest model level at the initial time.

166

167 Some modifications were made to the model for this study only in order to make the two  
168 microphysics schemes more directly comparable. The ~~calculation~~ diagnosis of saturation ratio  
169 from current values of the water vapor mixing ratio and temperature at the beginning of the  
170 microphysics routines was changed in the BULK scheme to make it the same as the calculation  
171 in the BIN. The BIN does not include a parameterization for aerosol dry deposition, so this  
172 process was turned off in the BULK scheme. Finally, the regeneration of aerosol upon droplet  
173 evaporation was deactivated in both microphysics schemes. Aerosol concentrations were  
174 initialized homogeneously in the horizontal and vertical directions. Aerosol particles did not  
175 interact with radiation.

176  
177 Five simulations were run with the BULK scheme and three with the BIN scheme. Since the  
178 relationships in Figure 1 (G98; RL03; MG07) suggest that the shape parameter may depend on  
179 the cloud droplet number concentration, the simulations were run with three different aerosol  
180 concentrations, specifically, 100, 400, and 1600  $\text{cm}^{-3}$ , in order to obtain a larger range of droplet  
181 concentration values. The aerosol in the BIN simulations was initialized with, and in the BULK  
182 simulations was assumed to follow, a lognormal distribution with a median radius of 40nm and a  
183 spectral width of 1.8. These BULK simulations used a shape parameter value of 4. Two  
184 additional BULK simulations were run with an aerosol concentration of 400  $\text{cm}^{-3}$  and shape  
185 parameter values of 2 and 7. These values were chosen based on previous analysis of the BIN  
186 simulations in Igel ~~et al.~~ and van den Heever 2016a 2017a. The BIN simulations will be referred  
187 to by the microphysics scheme abbreviation and the initial aerosol concentration, e.g. BIN100,  
188 and the BULK simulation names will additionally include the value of the cloud droplet shape  
189 parameter, e.g. BULK100-NU4.

190

## 191 4. Results

### 192 4.1 Instantaneous Condensation Rates

193 In order to compare directly the condensation rates predicted by the BULK and BIN  
194 microphysics schemes, it is necessary to evaluate these rates given the same thermodynamic and  
195 cloud microphysical conditions. The BULK condensation equation (Eq. (2)) is approximately  
196 linearly proportional to four quantities:  $S$ ,  $N_t$ ,  $\bar{D}$ , and  $v$ . We say approximately proportional since  
197 the presence of the ventilation coefficient (which itself depends on  $\bar{D}$  and  $v$ ) makes these factors  
198 not truly proportional to the condensation rate. In the BIN scheme, among these four variables,  
199 the condensation rate is only explicitly proportional to  $S$ , and is not explicitly proportional to  $N_t$ ,  
200  $\bar{D}$ , or  $v$  (which do not appear at all in Eq. (3)) since the BIN scheme does not make assumptions  
201 about the functional form of the size distribution. If it is assumed nevertheless that the BIN size  
202 distributions *can* be described by some probability distribution function (which does not  
203 necessarily have to be a gamma distribution), then we would still expect the BIN scheme  
204 condensation rate to scale linearly with  $N_t$  and  $\bar{D}$ .

205

206 Therefore, in order to best compare the condensation rates between the two schemes, the  
207 condensation and evaporation rates that occur during one time step were binned by the values of  
208  $S$ ,  $N_t$ , and  $\bar{D}$  that existed at the start of the condensation/evaporation process and were averaged  
209 in each bin. (Note that these phase space bins are not the same as the hydrometeor distribution  
210 bins.) That is, all points with the same  $S$ ,  $N_t$ , and  $\bar{D}$  were grouped and the average  
211 condensation or evaporation in each group of points was calculated. The average condensation  
212 rate in each  $S$ ,  $N_t$ , and  $\bar{D}$  joint bin was calculated separately for all simulations.

213  
214 Examples of the average condensation and evaporation rates from BIN400 are shown in Figure  
215 2a-b as functions of  $S$ ,  $N_t$ , and  $\bar{D}$ . Values in each joint bin differ for the other simulations. Where  
216 ~~the cloud was supersaturated or subsaturated,~~ saturation ratio bin widths of 0.1 or 1 were used  
217 where the cloud was supersaturated or subsaturated, respectively. For  $\bar{D}$ , bin widths of  $1 \mu\text{m}$   
218 were used. For  $N$ , the bin width depended on the initial aerosol concentration of the simulation:  
219 bin widths of 2.5, 10, and  $40 \text{ mg}^{-1}$  were used for simulations with an initial aerosol concentration  
220 of 100, 400, and  $1600 \text{ mg}^{-1}$ , respectively. The output from the dynamical model only includes  
221 the values of  $S$ ,  $N_t$ , and  $\bar{D}$  after condensation and evaporation have occurred. However, since the  
222 rates of condensation and droplet nucleation were known from additional model output, and  
223 since microphysics was the last physical process to occur during a time step in RAMS, the  $S$ ,  $N_t$   
224 and  $\bar{D}$  that existed before condensation occurred were easily calculated from the model output.  
225  
226 ~~Note that the aerosol activation parameterizations in the BULK and BIN microphysics were not~~  
227 ~~the same, and hence the number of nucleated cloud droplets was not the same. This impacted the~~  
228 ~~number of data points within each joint  $S$ ,  $N$ , and  $\bar{D}$  bin. However, we are primarily concerned~~  
229 ~~with the average condensation rate in each joint bin, and the average value should not be~~  
230 ~~impacted by the number of data points within a bin provided that the number is sufficiently high~~  
231 ~~(joint bins with fewer than 50 data points are neglected). Therefore, the differences in the aerosol~~  
232 ~~activation parameterizations, or for that matter, differences in the evolution of the cloud fields,~~  
233 ~~should not influence the differences in the average condensation rates as evaluated in our~~  
234 ~~framework.~~

235

236 ~~The average condensation rate in each  $S$ ,  $N$ , and  $\bar{D}$  joint bin was calculated for all simulations.~~  
237 All points where the cloud mixing ratio before condensation was greater than  $0.01 \text{ g kg}^{-1}$  and the  
238 cloud droplet number concentration was greater than  $5 \text{ mg}^{-1}$  were included in the analysis. ~~In~~  
239 ~~addition, grid points with relative humidity between 99% and 101% after condensation or~~  
240 ~~evaporation were excluded. The condensation or evaporation rates at these points was limited by~~  
241 ~~the supersaturation or subsaturation, respectively, and thus the rates were not highly dependent~~  
242 ~~on the droplet characteristics.~~ Finally, joint bins with fewer than 50 data points were discarded.  
243  
244 ~~Figure 2 shows an example of the average condensation and evaporation rates in the joint bins~~  
245 ~~for one simulation.~~ As is seen in Figure 2a-b, there is a smooth transition to higher condensation  
246 rates as the saturation ratio increases, and to higher condensation ( $S \geq 1$ ) and evaporation ( $S < 1$ )  
247 rates as the diameter or number mixing ratio increases. This is expected based on the  
248 condensation equations (Eqs. (2), (3)). All other simulations behave similarly.  
249  
250 Note that the aerosol activation parameterizations in the BULK and BIN microphysics were not  
251 the same, and hence the number of nucleated cloud droplets was not the same. This impacted the  
252 number of data points within each joint  $S$ ,  $N$ , and  $\bar{D}$  bin. However, we are primarily concerned  
253 with the average condensation rate in each joint bin, and the average value should not be  
254 impacted by the number of data points within a bin provided that the number is sufficiently high  
255 (joint bins with fewer than 50 data points are neglected). Therefore, the differences in the aerosol  
256 activation parameterizations, or for that matter, differences in the evolution of the cloud fields,  
257 should not influence the average condensation rates as evaluated in our framework.  
258

259 In order to compare easily the condensation rates predicted by the two microphysics schemes, we  
260 calculate the ratio of the average condensation/evaporation rate of each joint bin from a BULK  
261 simulation to the average condensation/evaporation rate of the corresponding joint bin from a  
262 BIN simulation, and then calculate the natural logarithm of each ratio. These will be referred to  
263 as ‘ln(ratios)’. ~~logarithm of the BULK to BIN condensation and evaporation rate ratios (these~~  
264 values will be referred to as ‘ln(ratios)’.We find the ln(ratios) of average  
265 condensation/evaporation rate for five pairs of simulations. Specifically, BULK400-NU2,  
266 BULK400-NU4, and BULK400-NU7 are all compared to BIN400, while BULK100-NU2 is  
267 compared to BIN100 and BULK1600-NU2 is compared to BIN1600. Histograms of the  
268 ln(ratios) ~~this ratio~~ for all pairs of simulations are shown in Figure 3a-b and Figure 3e-f. ~~This set~~  
269 ~~of ln(ratio) histograms will be referred to as ORIG.~~ The data have been separated into  
270 subsaturated (evaporating) and supersaturated (condensing) points. Positive values indicate that  
271 the rates in the BULK scheme are larger, and negative values indicate that the rates in the BIN  
272 scheme are larger. Values of  $\pm 0.1$  ( $\pm 0.2$ ) correspond to about a 10% (20%) difference in the  
273 condensation or evaporation rate between the two schemes for the joint bin.

274  
275 First we examine the impacts of increasing aerosol concentrations on the agreement of  
276 evaporation and condensation rates ~~for in~~ BULK and BIN simulations ~~with the same shape~~  
277 ~~parameter~~. Figures 3a-b show the histograms of the condensation and evaporation rate ln(ratios)  
278 for BULK100-NU4 compared to BIN100, BULK400-NU4 compared to BIN400, and  
279 BULK1600-NU4 compared to BIN1600 ~~pairs of simulations with a cloud droplet shape~~  
280 ~~parameter of 4 but with differing initial aerosol concentration~~. Figure 3a-3b reveals that in  
281 general the condensation rate is higher in the BIN scheme simulations as indicated by the more

282 frequent negative  $\ln(\text{ratios})$ .; ~~On the other hand, whereas~~ the evaporation rates are more similar  
283 between the two schemes as indicated by the most frequent  $\ln(\text{ratios})$  being ~~equaal~~ to or slightly  
284 greater than 0 in Figure 3a. ~~The evaporation rates are more frequently greater in the BULK~~  
285 ~~scheme simulations. For the simulation pair with an initial aerosol concentration of  $1600 \text{ cm}^{-3}$ ,~~  
286 ~~there is a long tail of positive  $\ln(\text{ratio})$  values. As a result, this pair of simulations has the highest~~  
287 ~~standard deviation of the  $\ln(\text{ratio})$  values of all simulation pairs (Table 2a).~~

288  
289 Figures 3e-f show the histograms of condensation and evaporation rate  $\ln(\text{ratios})$  for the three  
290 BULK400 simulations ~~that have~~with different values of the ~~cloud droplet~~ shape parameter, all  
291 compared to BIN400. ~~All three BULK400 simulations are compared to the BIN400 simulation.~~  
292 For both condensation and evaporation, the peak of the  $\ln(\text{ratios})$  histograms increase as the  
293 cloud droplet shape parameter used in the BULK400 simulations increases. For the BULK400-  
294 NU2 simulation, the condensation and evaporation rates are frequently 20% lower than the  
295 BIN400 rates or more whereas for the BULK400-NU7 simulation, the condensation rates  
296 compared to the BIN400 simulation are most frequently very similar ( $\ln(\text{ratios})$  near zero). Thus  
297 the value of the cloud droplet shape parameter chosen for use in a simulation is clearly important  
298 for determining how well a bulk microphysics scheme compares to a bin microphysics scheme in  
299 terms of predicted condensation and evaporation rates.

300

## 301 **4.2 Accounting for the Shape Parameter**

302 Fortunately, we know theoretically how the cloud droplet shape parameter will alter  
303 condensation and evaporation rates and this dependency can be accounted for in our comparison  
304 of the two microphysics schemes. The shape parameter term in Eq. (2) (hereafter  $f_{NU}$ ), which is

305 equal to  $\nu \left( \frac{\Gamma(\nu)}{\Gamma(\nu+3)} \right)^{1/3}$ , indicates that when a gamma PDF is assumed, the condensation rate is  
 306 proportional to the shape parameter  $\nu$  such that a higher shape parameter results in higher  
 307 condensation rates. ~~Of course, the BIN scheme makes no assumptions about the size~~  
 308 ~~distribution functionality and its condensation scheme does not depend on the shape parameter.~~  
 309 However, in order to characterize the shape of the predicted BIN cloud droplet size distributions,  
 310 and to facilitate the comparison of the BIN and BULK condensation rates, we assumed that the  
 311 predicted BIN size distributions are gamma PDF-like and found the best-fit gamma PDF  
 312 parameters (see Eq. (1)) for the cloud droplet size distributions at every cloudy grid point in the  
 313 BIN simulations. ~~We then evaluated the mean value of  $f_{NU}$  using these best-fit shape parameters~~  
 314 ~~for each joint bin in the  $S$ ,  $N$ , and  $\bar{D}$  phase space.~~

315  
 316 In order to find the best-fit shape parameters, we defined cloud droplets as belonging to one of  
 317 the first 15 bins of the BIN liquid array (the remaining 18 bins contain raindrops), which  
 318 corresponded to a maximum cloud droplet diameter of 50.8  $\mu\text{m}$ . Many methods are available to  
 319 find such best-fit parameters, but they generally all give similar results (McFarquhar et al.,  
 320 2014). Here we used the maximum-likelihood estimation (MLE) method. For our problem, the  
 321 log-likelihood function ( $\ln(L)$ ) is defined as

$$322 \quad \ln L = \frac{1}{N_t} \sum_{i=1}^{15} N_i \ln n(D_i) - \prod_{i=1}^{15} N(\text{bin}_i) \ln n(\text{bin}_i) \quad (4)$$

323 ~~where  $N(\text{bin}_i)$  is the simulated number concentration of cloud droplets in the  $i^{\text{th}}$  bin of the liquid~~  
 324 ~~size distribution array (each bin corresponds to a particular droplet diameter) and  $n(\text{bin}_i)n(D_i)$  is~~  
 325 ~~the value of the gamma PDF as defined in (Eq. 1) for  $D_i$  with unknown values of the parameters~~  
 326  ~~$D_n$  and  $\nu$ . The function is normalized by the total cloud droplet concentration  $N_t$  in order to~~  
 327 ~~remove  $N_t$  as a free parameter in Eq. 1. As indicated by its name, the MLE method seeks to~~

328 maximize the log-likelihood function given by Eq. 4. To do so, we used the MATLAB function  
329 fmincon to find the parameter values that minimized  $-1*L$ .and found best fits that minimize the  
330 error in the total number concentration. Using this method, the size distributions were first  
331 normalized by the corresponding total number concentration, leaving only  $D_n$  and  $v$  as free  
332 parameters of the distribution (Eq. 1).

333  
334 Note that while we could determine the values of  $S$ ,  $N_L$ , and  $\bar{D}$  that existed before condensation  
335 occurred, we could not determine the value of the best-fit shape parameter for this time because  
336 the change in mixing ratio of each bin was not output by RAMS. Thus, the average shape  
337 parameters used in the analysis are those that exist at the end of the time step. Nonetheless, given  
338 the short time step used in these simulations, it was not expected that the best-fit shape parameter  
339 would change much in one time step in most cases. The exception may be for very broad  
340 distributions characterized by low shape parameters. In part due to this concern, cloudy points  
341 with best-fit shape parameters less than 1 are not included in the analysis. This criterion  
342 eliminated 4.5%, 5.1%, and 8.6% of the data in BIN100, BIN400, and BIN1600, respectively.  
343 Overall, the impact of using the post-condensation shape parameters is not expected to have a  
344 large impact on the results. Examples of the average shape parameters in each joint bin are  
345 shown in Figure 2c-d. The shape parameter tends to increase with droplet concentration and be  
346 low (5 or less) for relative humidity less than 99%. In depth analysis of the best-fit shape  
347 parameter in the BIN simulations is found in Igel and van den Heever (2017a).

348  
349 Using these best-fit shape parameters from the BIN simulations and the specified shape  
350 parameters from the BULK simulations, ~~T~~the shape parameter term ( $f_{NU}$ ) can be evaluated for

351 each cloudy point for all simulations. joint bin in the  $S$ ,  $N$ , and  $\bar{D}$  phase space for all simulations.  
 352 In the case of each BULK simulations, the value of  $f_{NU,BULK} f_{NU}$  is the same for every joint  
 353 bin cloudy point since the value of  $f_{NU,BULK} f_{NU}$  is uniquely determined by the choice of the shape  
 354 parameter value for each BULK simulation. Specifically,  $f_{NU,BULK} = 0.69, 0.81,$  and  $0.88$  for  
 355 NU2, NU4, and NU7 simulations, respectively. For the BIN simulations,  $f_{NU,BIN} f_{NU}$  can be  
 356 calculated using the best-fit shape parameters and will have a different value for every cloudy  
 357 grid point. The values of  $f_{NU,BIN}$  for the cloudy grid points in each joint bin were averaged  
 358 together to find a mean  $\overline{f_{NU,BIN}}$  for each joint  $S$ ,  $N$ , and  $\bar{D}$  bin for each BIN simulation. Example  
 359 values of  $\overline{f_{NU,BIN}}$  for some joint bins are shown in Figure 2e-d2e-f. Unlike for the BULK  
 360 simulations, the value of  $f_{NU}$  for the BIN simulations will vary amongst the joint bins since the  
 361 best-fit shape parameter is determined from the freely evolving cloud droplet distributions that  
 362 are predicted by the BIN microphysics scheme. We can use the values of  $f_{NU,BULK} f_{NU}$  and  
 363  $\overline{f_{NU,BIN}}$  in our comparison of the condensation and evaporation rates to account for the  
 364 differences in condensation and evaporation rates between the two schemes that arise due to  
 365 different size distribution widthsshape parametersthe fact that the best-fit shape parameters in the  
 366 BIN simulations will often be different from the single prescribed value in the BULK  
 367 simulations. Specifically, in our analysis, we adjusted the mean condensation and evaporation  
 368 rates ( $C$ ) for each joint bin from the BULK simulations in the following way:

$$369 \quad \overline{C_{BULK,corrected}} C_{BULK,corrected} = \overline{C_{BULK,original}} C_{BULK,original} \frac{\overline{f_{NU,BIN}} f_{NU,BIN}}{f_{NU,BULK}} \quad (45)$$

370 Note again that the value of  $\overline{f_{NU,BIN}} f_{NU,BIN}$  will be different for each joint bin. By making this  
 371 correction, we found the condensation and evaporation rates that the BULK simulations *would*  
 372 *have had* if they had used the same value of the shape parameter that best characterized the cloud

373 droplet size distributions that were predicted by the BIN simulations. To be clear, we did not run  
374 new simulations, rather the outputted condensation/evaporation rates from the existing BULK  
375 simulations were adjusted for the purposes of our analysis using Eq. 45 to account for the  
376 differences in size distribution shapes between the BIN and BULK simulations. We will next  
377 compare these adjusted BULK condensation/evaporation rates to the BIN rates to see if the  
378 comparison improves.

379  
380 The  $\ln(\text{ratios})$  of the ~~modified-adjusted~~ condensation and evaporation rates from the BULK  
381 simulations to the rates from the BIN simulations are shown in Figures 3c-d and Figures 3g-h.  
382 Hereafter, these  $\ln(\text{ratios})$  will be called adjusted  $\ln(\text{ratios})$ . This set of  $\ln(\text{ratios})$  will be referred  
383 to as CORR. The most frequent value of the ~~CORR-adjusted~~  $\ln(\text{ratios})$  is near zero (indicating  
384 that the two schemes predict the same rate) for all simulation pairs and for both condensation and  
385 evaporation. The impact of the ~~modification-adjustment~~ is most notable in Figures 3g-h where  
386 the histograms of the ~~CORR-adjusted~~  $\ln(\text{ratios})$  now nearly lie on top of one another whereas in  
387 Figures 3e-f they are clearly separated. Thus, it appears that our method of accounting for the  
388 value of the shape parameter has worked well.

389  
390 ~~Furthermore~~ Additionally, the standard deviations of the ~~condensation rate-CORR-adjusted~~  
391  $\ln(\text{ratio})$  histograms (shown in the legend of each panel) for condensation is-are decreased by  
392 about half compared to the ORIG  $\ln(\text{ratio})$  histograms (Table 2a-b) slightly. This is not the case  
393 for the ~~evaporation rate-CORR-adjusted~~  $\ln(\text{ratio})$  histograms for evaporation, where for in four out  
394 of five all simulation pairs the standard deviation is increased compared to the ~~ORIG-original~~  
395  $\ln(\text{ratio})$  histograms. Nonetheless, given that all ~~CORR-adjusted~~ histograms (Fig. 3c-d, g-h) now

396 have a modal value near 0, whereas this was not the case with the ~~ORIG-original~~ histograms  
397 (Fig. 3a-b, e-f), the shape parameter appears to be the primary reason why the condensation and  
398 evaporation rates in the two schemes do not always agree.

399

## 400 **4.3 Other Considerations**

401 While the shape parameter appears to be the primary cause of differences in condensation  
402 and evaporation rates in bin and bulk microphysics schemes, it is worth investigating whether  
403 other factors are important.

404

### 405 **4.3.1 Relative Humidity**

406 When the relative humidity is close to 100%, the condensation and evaporation rates  
407 should be limited by the small supersaturation or subsaturation. In these situations, the droplet  
408 properties are expected to have little impact on the condensation or evaporation rate. Instead,  
409 these rates will be largely determined by how the schemes behave when the time scale for  
410 condensation or evaporation is smaller than the time step of the model. Figure 4 shows the  
411 average and standard deviation of the adjusted ln(ratios) for all five pairs of simulations as a  
412 function of relative humidity. Both the average and the standard deviation peak for relative  
413 humidity near 100%. This indicates that the agreement between the bulk and bin schemes on  
414 condensation/evaporation rates scheme is poor, just as we expected it to be based on the above  
415 arguments. That said, condensation and evaporation rates occurring with relative humidity near  
416 100% are small in magnitude, and disagreements here are not expected to have a large impact on  
417 the simulation evolution. treat

418 We repeated the analysis shown in Figure 3, but excluding data points where the relative  
419 humidity before condensation/evaporation was between 99.5% and 100.5%. The results are  
420 shown in Figure 5. Qualitatively, the results in Figures 3 and 5 are similar. The adjusted  
421 histograms are all centered near 0, but ~~The reduction in the decrease in the standard deviation of~~  
422 the ln(ratios) (shown in the legends) from Figure 3 to Figure 5 is substantial, ~~particularly for~~  
423 condensation. This indicates that by removing cloudy points with relative humidity between  
424 99.5% and 100.5%, the agreement between the two schemes increases. That said, the standard  
425 deviations of the ~~corrected~~ adjusted evaporation histograms are still higher than those of the  
426 original ~~unadjusted~~ histograms. Finally, unlike in Figure 3, ~~After the shape parameter correction~~  
427 is applied (Fig. 5c, d, g, h), the standard deviation for the adjusted condensation histograms is  
428 consistently lower than that of the ~~adjusted~~ evaporation histograms. Thus ~~Overall, it seems that~~  
429 the correction based on the shape parameter for condensation is more successful than that for  
430 evaporation in terms of the spread of ln(ratios). Potential reasons for this difference are explored  
431 next.

#### 434 **4.3.1.2 Appropriateness of the Gamma PDF and Fractional Mass Change**

435 One potential ~~factor~~ reason worth considering is that the gamma PDF is not always  
436 appropriate for characterizing the cloud droplet size distributions in the BIN simulations. The  
437 BIN microphysics scheme is capable of predicting any shape for the cloud droplet size  
438 distributions, including size distributions that may be bimodal. To assess how well our fitted  
439 gamma PDFs approximated the actual simulated cloud droplet size distributions, we calculated  
440 the normalized root mean square error (NRMSE) of the fits using MATLAB's goodnessOfFit

441 function. An NRMSE of 1 indicates that the fit was no better than a ~~straight~~flat line equal to the  
442 mean of the data size distribution, and a value of 0 indicates a perfect fit. Figures ~~4a~~6a-b show  
443 cumulative histograms of the NRMSE values from the three BIN simulations for both  
444 evaporating and condensing cloudy points. Note that these are not cumulative histograms of  
445 mean values from joint bins as in Figure 3 but rather they are cumulative histograms of the  
446 NRMSE values at all individual cloudy grid points in the BIN simulations. The majority of grid  
447 points have NRMSE values between about 0.4 and 0.6 ~~or lower~~ which indicates that in  
448 general the gamma PDF characterizes the simulated cloud droplet size distributions ~~very~~  
449 moderately well. The cumulative distributions of NRMSE are similar for all three BIN  
450 simulations and similar for evaporating and condensing cloudy grid points. This suggests that the  
451 NRMSE probably cannot explain why the correction in Figure 5 leads to a reduction in the  
452 standard deviation of  $\ln(\text{ratios})$  for condensation but an increase in the standard deviation of  
453  $\ln(\text{ratios})$  for evaporation. Nonetheless, we still expect that higher NRMSE should result in  
454 differences between the condensation and evaporation rates in bin and bulk schemes. This will  
455 be discussed further below.

456  
457 ~~We repeated the calculations of mean condensation or evaporation rate in each  $S$ ,  $N$ , and  $\bar{D}$  joint~~  
458 ~~bin for the BIN simulations, but now we only included those cloudy points with an NRMSE of~~  
459 ~~0.6 or more (those points with a poor gamma PDF fit). The joint bins for the BULK simulations~~  
460 ~~were unaltered, but did include the modification described by Eq. (4) which now used values of~~  
461  ~~$f_{NU, BIN}$  based only on the high NRMSE points. The resulting histograms of condensation and~~  
462 ~~evaporation rate  $\ln(\text{ratios})$  are shown in Figures 5a-b for all simulation pairs. The associated~~  
463 ~~standard deviations are listed in Table 2c. This set of histograms will be referred to as CORR-~~

464 ~~POOR. For evaporation, the peaks of the CORR-POOR  $\ln(\text{ratios})$  histograms shift to positive~~  
465 ~~values (Fig. 5a) indicating that the agreement between the BULK and BIN rates is degraded,~~  
466 ~~although the standard deviations of these histograms are similar compared to the CORR~~  
467 ~~histograms (Table 2c compared to Table 2b). The shift in peak  $\ln(\text{ratios})$  suggests that when the~~  
468 ~~BIN simulations produce cloud droplet size distributions that poorly conform to a gamma PDF,~~  
469 ~~the best-fit shape parameter is less useful for understanding the differences between BULK and~~  
470 ~~BIN evaporation rates.~~

471  
472 ~~However, for condensation rates, the results are less clear. Figure 5b shows that many of the high~~  
473 ~~CORR-POOR  $\ln(\text{ratio})$  histograms are still centered near 0, which indicates that the BIN and~~  
474 ~~modified BULK condensation rates still agree well. Furthermore, the standard deviation of these~~  
475 ~~histograms is similar those of the CORR histograms (Table 2b-c). Unlike for evaporation, these~~  
476 ~~results for condensation suggest that the fact that the BIN simulations do not predict cloud~~  
477 ~~droplet size distributions that are similar to gamma PDFs is not an important reason why the~~  
478 ~~BULK and BIN schemes predict different condensation rates. It is unclear why the comparisons~~  
479 ~~of condensation and evaporation rates behave so differently. This uncertainty will be explored~~  
480 ~~next.~~

481  
482 Another 4.3.2 Fraction of Cloud Mass Evaporated

483 ~~One~~ potential reason that evaporation ~~comparison is generally worse than the~~ and condensation  
484 comparisons are different relates to the fractional change of mass. Specifically, the comparison  
485 may be better for situations in which only a small fraction of the total cloud droplet mass is  
486 ~~condensed or~~ evaporated or condensed within a time step versus a situation in which a large

487 fraction of mass is evaporated or condensed. The reason the fractional change in mass may be  
488 important is related to the different treatments of the time step during condensation/evaporation  
489 in the two schemes. is that†The BIN microphysics scheme takes an iterative approach to  
490 condensation and evaporation in which many small steps are taken. After each small step the  
491 droplet properties are updated. When the droplet properties are changing rapidly, this approach  
492 may be important for accurately predicting the evolution of the total mass and number of cloud  
493 droplets. On the other hand, the RAMS bulk scheme takes just one step (which is equal to the  
494 full model time step length) and cannot account for rapidly changing droplet properties within  
495 the time step.

496

497 Cumulative histograms of the fraction of cloud mass evaporated in one full time step is shown in  
498 Figure 4e-6c for the BIN simulations. Higher fractions of mass are evaporated more frequently as  
499 the initial aerosol concentration increases. This result is not surprising given that the high  
500 numbers of cloud droplets nucleated from the high numbers of aerosol particles will induce on  
501 average higher evaporation rates (Eq (2) and Eq (3)) that cause a higher fraction of mass to be  
502 evaporated in one time step. Similarly, cumulative histograms of the fraction of cloud droplet  
503 mass condensed in the time step are shown in Figure 4d6d. Again, high fractions of cloud mass  
504 are condensed more frequently as the initial aerosol concentration increases. ~~Overall~~In general,  
505 large fractional changes in the cloud mass are more frequent during evaporation during  
506 condensation. This suggests that the fractional mass change may be a reason for the better  
507 comparison of condensation rates than evaporation rates in Figure 5 after the shape parameter  
508 correction was applied.

509

510 To explore simultaneously the impact of NRMSE and fractional mass change on the comparison  
511 of bin and bulk scheme condensation and evaporation rates, we also calculated the mean  
512 NRMSE and fractional mass change of each of the joint  $S$ ,  $N_r$ , and  $\bar{D}$  bins in addition to the  
513 adjusted ~~mean~~-ln(ratio) for each bin that we have shown previously. In this analysis, we have  
514 excluded points with relative humidity between 99.5% and 100.5% based on our previous  
515 analysis of the impact of relative humidity. Joint bins with similar mean NRMSE and fractional  
516 mass change were grouped together ~~to find~~ and the mean of the adjusted ~~mean~~-ln(ratios) for  
517 each group was calculated. Joint bin pairss from all simulation pairs were included. The results  
518 are shown in Figure 7, again for condensation and evaporation separately, where colors show the  
519 mean of the adjusted ~~mean~~-ln(ratios) as a function of NRMSE and fractional mass change.  
520 Colors near zero (teal) indicate that the two schemes agree well after the shape parameter  
521 correction is applied, whereas colors away from zero (blue and yellow) indicate that the two  
522 schemes do not agree well even after the shape parameter ~~correction~~adjustment is applied.  
523  
524 Evaporation will be considered first (Fig. 7a). For ~~fraction of mass evaporated~~evaporated mass  
525 fraction less than about 0.3, the mean adjusted ~~mean~~-ln(ratios) are near zero. As the ~~fraction of~~  
526 ~~mass evaporated~~evaporated mass fraction increases above 0.3, the NRMSE also begins to  
527 increase, which makes it difficult to understand the influence of either the NRMSE or evaporated  
528 mass fraction on the scheme comparison by looking at them in isolation. However, by looking at  
529 them together in Figure 7a, we see that the evaporated mass fraction seems to be driving the  
530 increase in the adjusted mean ln(ratio) away from 0, particularly when the evaporated mass  
531 fraction is greater than 0.4. For these values, the contour lines are approximately flat, which  
532 indicates that there is little dependence of the mean adjusted ln(ratios) on NRMSE.

533  
534 The NRMSE seems to be more important for condensation than evaporation. As the NRMSE  
535 increases above about 0.5 in Figure 7b for condensation, the mean adjusted  $\ln(\text{ratios})$   
536 begins to drop away from zero, and the two schemes have worse agreement on the condensation  
537 rates which indicates that the bin scheme is predicting higher condensation rates than the bulk  
538 scheme. Like for evaporation, when NRMSE and the condensed mass fraction are both relatively  
539 low, the mean adjusted  $\ln(\text{ratios})$  are near zero and show little dependence on NRMSE or  
540 fractional mass change.

541 ~~Again, the calculations of mean evaporation rate in each  $S$ ,  $N$ , and  $\bar{D}$  joint bin for both the BULK~~  
542 ~~and BIN simulations were repeated but this time with cloudy points separated by low and high~~  
543 ~~mass fraction change. High evaporated mass fraction is defined as 0.25 or higher. Very few~~  
544 ~~cloudy points undergoing condensation have a mass fraction change of 0.25 or higher. Likewise,~~  
545 ~~very few evaporating cloudy points in BIN100 exceed this threshold. Thus, the analysis is only~~  
546 ~~performed for the subsaturated, evaporating cloudy points for simulations pairs that include~~  
547 ~~BIN400 or BIN1600.~~

548  
549 ~~The evaporation rate  $\ln(\text{ratio})$  histograms for the two groups (referred to as CORR-LFR and~~  
550 ~~CORR-HFR) are shown in Figures 5c-d and the associated standard deviations are listed in Table~~  
551 ~~2d-e. It is immediately obvious that the two microphysics schemes behave quite differently for~~  
552 ~~the case of high evaporated fractions. The standard deviation of the CORR-HFR  $\ln(\text{ratio})$~~   
553 ~~histograms are up to twice as large as those for ORIG or CORR-LFR (Table 2a,d). Furthermore,~~  
554 ~~most of the CORR-HFR histograms are shifted almost entirely to the right of 0. This result~~  
555 ~~indicates that when the BIN simulations evaporate a high fraction of the cloud mass in one time~~

556 ~~step, they almost always predict a higher evaporation rate than the BULK simulations when~~  
557 ~~given the same initial cloud properties and relative humidity.~~  
558  
559 ~~Finally, we found that grid points at which a high fraction of cloud mass is evaporated, the cloud~~  
560 ~~droplet size distributions predicted by the BIN simulations are more likely to fit poorly to a~~  
561 ~~gamma PDF (not shown). Thus, we performed the BULK to BIN evaporation rate comparison~~  
562 ~~twice more: firstly where only BIN simulation points with a high NRMSE of the fitted gamma~~  
563 ~~distributions and a low fraction of cloud mass evaporated were included, and secondly with the~~  
564 ~~opposite conditions where only BIN simulations points with a low NRMSE and a high~~  
565 ~~evaporated fraction were included. The standard deviations of the resultant histograms are listed~~  
566 ~~in Table 2f-g. In the case of high NRMSE and low evaporated fraction, the standard deviations~~  
567 ~~are similar to those for CORR (Table 2b,f), whereas in the case of low NRMSE and high~~  
568 ~~evaporated fraction the standard deviations are high and are similar to those for CORR-HFR.~~  
569 ~~Thus, it seems that the occurrence of high evaporated fraction is more important for explaining~~  
570 ~~poor agreement between the BULK and BIN microphysics scheme than is a poor fit of a gamma~~  
571 ~~PDF to the cloud droplet size distributions simulated by the BIN scheme.~~

572

## 573 **5. Conclusions**

574 In this study, we have compared the cloud condensation rates predicted by a bulk and a bin  
575 microphysics scheme in simulations of non-precipitating cumulus clouds run using the same  
576 dynamical framework, namely RAMS. The simulations were run with three different background  
577 aerosol concentrations in order to consider a large range of microphysical conditions. Two

578 additional simulations with the RAMS bulk microphysics scheme were run with different  
579 settings for the cloud droplet shape parameter.

580  
581 When the condensation and evaporation rates were binned by saturation ratio, cloud droplet  
582 number concentration, and mean diameter, the BULK rates were on average higher or lower  
583 depending primarily on the value of the shape parameter used in the BULK simulations. Since  
584 the theoretical relationship between the shape parameter and condensation/evaporation rates is  
585 known, we adjusted the BULK rates to be those that the simulations would have predicted if they  
586 had used the same value of the shape parameter as was found by fitting gamma PDFs to the BIN  
587 droplet size distribution output. After doing so, we showed that the BULK and BIN rates were in  
588 general in much better agreement, although the condensation rates agreed better than the  
589 evaporation rates. After mathematically accounting for the fixed shape parameter assumed for  
590 BULK cloud droplet size distributions, we showed that the BULK and BIN rates were in general  
591 in much better agreement, although the condensation rates agreed better than the evaporation  
592 rates.

593  
594 Other factors were also suggested to impact the agreement of condensation and evaporation rates  
595 in the BIN and BULK simulations. First, the agreement was worse as the relative humidity  
596 approached 100%. Second, the when the simulated binned size distributions did not conform  
597 closely to a gamma PDF (NRMSE was high), the agreement was also worse, particularly for  
598 condensation. Lastly, when ~~Additional analysis supported the following conclusions:~~

599 1. ~~A gamma probability distribution appears to be a good assumption for the cloud droplet~~  
600 ~~distribution shape, and the exact knowledge of the distribution shape in a bin scheme is often not~~  
601 ~~necessary to minimize errors in the condensation rate in bulk schemes.~~

602 ~~When a large fraction of the cloud droplet population mass was evaporated or condensed within~~  
603 ~~a model time step, the agreement was also worse, particularly for evaporation. We hypothesize~~  
604 ~~that the reason for a dependence on the fractional mass change is related to the different~~  
605 ~~approaches taken by the BIN and BULK schemes to solve the condensation equation. the BIN~~  
606 ~~scheme usually predicts lower evaporation rates than the BULK scheme. This appears to be one~~  
607 ~~reason why the evaporation rates comparison is poorer than the condensation rates comparison. It~~  
608 ~~is possible that the multiple sub-time steps taken by the BIN scheme may be important for~~  
609 ~~accurately predicting evaporation rates. Such a time-stepping approach could easily be~~  
610 ~~implemented in a BULK scheme. This reason for disagreement between the two schemes,~~  
611 ~~however, is of secondary importance compared to the shape parameter. However, all three of~~  
612 ~~these factors were found to be of secondary importance compared to the shape parameter.~~

613 2.

614 Again, it appears that when the relative humidity is not near 100%, the most important factor for  
615 agreement in cloud droplet condensation and evaporation rates between bin and bulk schemes is  
616 the shape of the cloud droplet size distribution. Therefore, we feel that MmoreMore effort is  
617 needed to understand ~~the behavior of~~ the cloud droplet shape parameter in order to improve the  
618 representation of cloud droplet size distributions in bulk microphysics schemes. Improvement in  
619 the representation of size distributions should lead to better agreement in the simulated  
620 macroscopic properties of clouds by the two schemes, although such potential for better  
621 agreement has not been shown here. Finally, while the methods we have used to here to

622 demonstrate the importance of the shape parameter were effective, we are not suggesting that the  
623 same methods would be best for improving bulk schemes. and ultimately improve the  
624 simulations of clouds.

625  
626 Although we have only investigated two specific schemes, it is expected that the results can be  
627 applied more generally to ~~bulk-bin~~ and ~~bulk-in~~ schemes that do not use saturation adjustment.  
628 Additional work should be conducted using a similar approach in order to compare and evaluate  
629 additional microphysics schemes and additional microphysical processes. While it is clear that  
630 the ~~effective~~-shape parameter ~~in the bin simulations~~ explains much of the discrepancies in  
631 predicted condensation rates between bin and bulk schemes, our understanding of what the most  
632 appropriate value of the shape parameter is or how it should vary as a function of basic cloud  
633 properties is limited. More work then is also needed ~~to on~~ understanding cloud droplet  
634 distribution widths from observations and measurements.

#### 636 **Acknowledgements:**

637 The authors thank Alexander Khain for generously sharing his BIN code in order to make this  
638 study possible. This material is based on work supported by the National Science Foundation  
639 Graduate Research Fellowship Program under Grant No. DGE-1321845 and the National  
640 Aeronautics and Space Administration Grant No. NNX13AQ32G. Additional information can be  
641 found in the supporting information or be requested from the corresponding author.

#### 643 **Appendix A**

#### 644 **Implementation of the Hebrew University BIN scheme into RAMS**

645  
646  
647  
648  
649  
650  
651  
652  
653  
654  
655  
656  
657  
658  
659  
660  
661  
662  
663  
664  
665  
666  
667

While the present study is only concerned with warm phase processes, the methods to interface the Hebrew University BIN scheme with the RAMS radiation scheme (Harrington, 1997) will be described here, ~~including those for the ice species~~. The RAMS radiation scheme uses pre-computed lookup tables for the extinction coefficient, single-scattering albedo, and asymmetry parameter for each hydrometeor species. ~~Three of the hydrometeor species in the BIN correspond directly to species in the RAMS microphysics scheme, namely, aggregates, graupel, and hail.~~ All liquid drops are represented as one species in the BIN, so these liquid bins are classified as either cloud droplets or rain drops using the same size threshold used by the RAMS microphysics scheme to distinguish these two species. ~~Finally, the BIN represents three ice crystal types—plates, columns, and dendrites. Separate RAMS radiation look-up tables already exist for these different ice crystal types, but like for cloud and rain, there are two tables for each crystal type depending on the mean size of the crystals. In RAMS, the small ice crystals are referred to as pristine ice, and the large ice crystals as snow. Again, the same size threshold used to distinguish these two ice categories is used to assign bins from the BIN ice crystal species as either pristine ice or snow. This fortuitous overlap in the ice species has allowed for the seamless integration of the BIN hydrometeor species with the RAMS radiation scheme.~~ For each set of BIN bins that corresponds to a RAMS species, the total number concentration and mean diameter is calculated, a gamma distribution shape parameter of 2 is assumed, and the appropriate set of look-up tables for the corresponding RAMS species is used for all radiative calculations.

**References:**

668 [Beheng, K. D.: A parameterization of warm cloud microphysical conversion processes, Atmos.](#)  
669 [Res., 33, 193–206, doi:10.1016/0169-8095\(94\)90020-5, 1994.](#)  
670  
671 [Grabowski, W. W.: Toward Cloud Resolving Modeling of Large-Scale Tropical Circulations: A](#)  
672 [Simple Cloud Microphysics Parameterization, J. Atmos. Sci., 55\(21\), 3283–3298,](#)  
673 [doi:10.1175/1520-0469\(1998\)055<3283:TCRMOL>2.0.CO;2, 1998.](#)  
674  
675 [Harrington, J. Y.: The effects of radiative and microphysical processes on simulation of warm](#)  
676 [and transition season Arctic stratus, Colorado State University., 1997.](#)  
677  
678 [Igel, A. L. and van den Heever, S. C.: The Importance of the Shape of Cloud Droplet Size](#)  
679 [Distributions in Shallow Cumulus Clouds. Part I: Bin Microphysics Simulations. J. Atmos. Sci.](#)  
680 [74, 249-258, doi:10.1175/JAS-D-15-0382.1.](#)  
681  
682 [Igel, A. L. and van den Heever, S. C.: The Importance of the Shape of Cloud Droplet Size](#)  
683 [Distributions in Shallow Cumulus Clouds. Part II: Bulk Microphysics Simulations. J. Atmos.](#)  
684 [Sci. 74, 259-273, doi:10.1175/JAS-D-15-0383.1.](#)  
685  
686 [Khain, A., Pokrovsky, A., Pinsky, M., Seifert, A. and Phillips, V.: Simulation of Effects of](#)  
687 [Atmospheric Aerosols on Deep Turbulent Convective Clouds Using a Spectral Microphysics](#)  
688 [Mixed-Phase Cumulus Cloud Model. Part I: Model Description and Possible Applications, J.](#)  
689 [Atmos. Sci., 61\(24\), 2963–2982, doi:10.1175/JAS-3350.1, 2004.](#)  
690

691 [Khain, A. P. and Sednev, I.: Simulation of precipitation formation in the Eastern Mediterranean](#)  
692 [coastal zone using a spectral microphysics cloud ensemble model, Atmos. Res., 43\(1\), 77–110,](#)  
693 [doi:10.1016/S0169-8095\(96\)00005-1, 1996.](#)  
694  
695 [Khain, A. P., Beheng, K. D., Heymsfield, A., Korolev, A., Krichak, S. O., Levin, Z., Pinsky, M.,](#)  
696 [Phillips, V., Prabhakaran, T., Teller, A., van den Heever, S. C. and Yano, J.-I.: Representation of](#)  
697 [microphysical processes in cloud-resolving models: Spectral \(bin\) microphysics versus bulk](#)  
698 [parameterization, Rev. Geophys., 53\(2\), 247–322, doi:10.1002/2014RG000468, 2015.](#)  
699  
700 [Kumjian, M. R., Ganson, S. M. and Ryzhkov, A. V.: Freezing of Raindrops in Deep Convective](#)  
701 [Updrafts: A Microphysical and Polarimetric Model, J. Atmos. Sci., 69\(12\), 3471–3490,](#)  
702 [doi:10.1175/JAS-D-12-067.1, 2012.](#)  
703  
704 [McFarquhar, G. M., Hsieh, T.-L., Freer, M., Mascio, J. and Jewett, B. F.: The Characterization](#)  
705 [of Ice Hydrometeor Gamma Size Distributions as Volumes in  \$N\_0 - \lambda - \mu\$  Phase Space:](#)  
706 [Implications for Microphysical Process Modeling, J. Atmos. Sci., 72\(2\), 892–909,](#)  
707 [doi:10.1175/JAS-D-14-0011.1, 2015.](#)  
708  
709 [Milbrandt, J. A. and McTaggart-Cowan, R.: Sedimentation-Induced Errors in Bulk Microphysics](#)  
710 [Schemes, J. Atmos. Sci., 67\(12\), 3931–3948, doi:10.1175/2010JAS3541.1, 2010.](#)

711

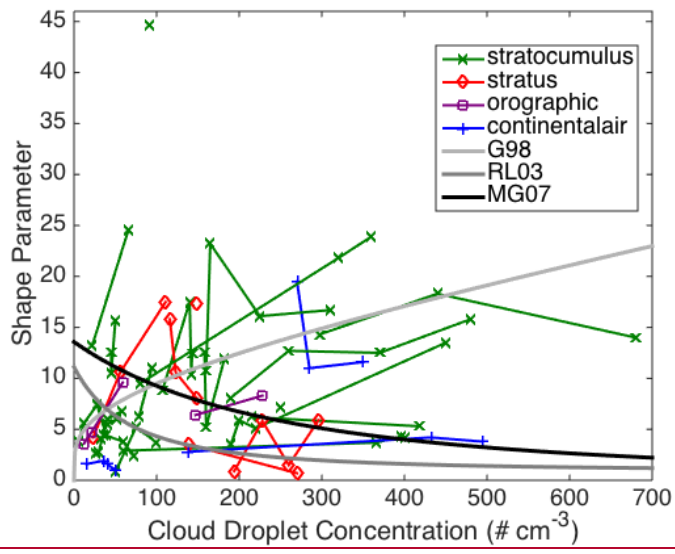
712 [Milbrandt, J. A. and Yau, M. K.: A Multimoment Bulk Microphysics Parameterization. Part I:](#)  
713 [Analysis of the Role of the Spectral Shape Parameter, J. Atmos. Sci., 62\(9\), 3051–3064,](#)  
714 [doi:10.1175/JAS3534.1, 2005.](#)  
715  
716 [Miles, N. L., Verlinde, J. and Clothiaux, E. E.: Cloud Droplet Size Distributions in Low-Level](#)  
717 [Stratiform Clouds, J. Atmos. Sci., 57\(2\), 295–311, doi:10.1175/1520-](#)  
718 [0469\(2000\)057<0295:CSDIL>2.0.CO;2, 2000.](#)  
719  
720 [Morrison, H. and Grabowski, W. W.: Comparison of Bulk and Bin Warm-Rain Microphysics](#)  
721 [Models Using a Kinematic Framework, J. Atmos. Sci., 64\(8\), 2839–2861, doi:10.1175/JAS3980,](#)  
722 [2007.](#)  
723  
724 [Rotstayn, L. D. and Liu, Y.: Sensitivity of the First Indirect Aerosol Effect to an Increase of](#)  
725 [Cloud Droplet Spectral Dispersion with Droplet Number Concentration, J. Clim., 16\(21\), 3476–](#)  
726 [3481, doi:10.1175/1520-0442\(2003\)016<3476:SOTFIA>2.0.CO;2, 2003.](#)  
727  
728 [Saleeby, S. M. and Cotton, W. R.: A Large-Droplet Mode and Prognostic Number Concentration](#)  
729 [of Cloud Droplets in the Colorado State University Regional Atmospheric Modeling System](#)  
730 [\(RAMS\). Part I: Module Descriptions and Supercell Test Simulations, J. Appl. Meteorol., 43\(1\),](#)  
731 [182–195, doi:10.1175/1520-0450\(2004\)043<0182:ALMAPN>2.0.CO;2, 2004.](#)  
732

733 [Saleeby, S. M. and van den Heever, S. C.: Developments in the CSU-RAMS Aerosol Model:](#)  
734 [Emissions, Nucleation, Regeneration, Deposition, and Radiation, J. Appl. Meteorol. Climatol.,](#)  
735 [52\(12\), 2601–2622, doi:10.1175/JAMC-D-12-0312.1, 2013.](#)  
736  
737 [Seifert, A. and Beheng, K. D.: A double-moment parameterization for simulating](#)  
738 [autoconversion, accretion and selfcollection, Atmos. Res., 59-60, 265–281, doi:10.1016/S0169-](#)  
739 [8095\(01\)00126-0, 2001.](#)  
740  
741 [Walko, R. L., Cotton, W. R., Feingold, G. and Stevens, B.: Efficient computation of vapor and](#)  
742 [heat diffusion between hydrometeors in a numerical model, Atmos. Res., 53\(1-3\), 171–183,](#)  
743 [doi:10.1016/S0169-8095\(99\)00044-7, 2000.](#)  
744  
745 [Zhu, P. and Albrecht, B.: Large eddy simulations of continental shallow cumulus convection, J.](#)  
746 [Geophys. Res., 108\(D15\), 4453, doi:10.1029/2002JD003119, 2003.](#)

	(a) Original, all data (ORIG)	(b) Corrected, all data (CORR)	(c) Corrected, high NRMSE only (CORR-POOR)	(d) Corrected, low fraction mass evaporated (CORR-LFR)	(e) Corrected, high fraction mass evaporated (CORR-HFR)	(f) Corrected, high NRMSE and low fraction evaporated
<b>Evaporation</b>						
BULK100-NU4/BIN100	0.032	0.025	0.025	-	-	-
BULK400-NU4/BIN400	0.044	0.055	0.056	0.041	0.056	0.038
BULK1600-NU4/BIN1600	0.097	0.120	0.134	0.090	0.160	0.105
BULK400-NU2/BIN400	0.041	0.054	0.053	0.053	0.046	0.041
BULK400-NU7/BIN400	0.061	0.072	0.064	0.047	0.087	0.041
<b>Condensation</b>						
BULK100-NU4/BIN100	0.057	0.033	0.027	-	-	-
BULK400-NU4/BIN400	0.056	0.027	0.035	-	-	-
BULK1600-NU4/BIN1600	0.057	0.033	0.032	-	-	-
BULK400-NU2/BIN400	0.059	0.029	0.032	-	-	-
BULK400-NU7/BIN400	0.050	0.026	0.023	-	-	-

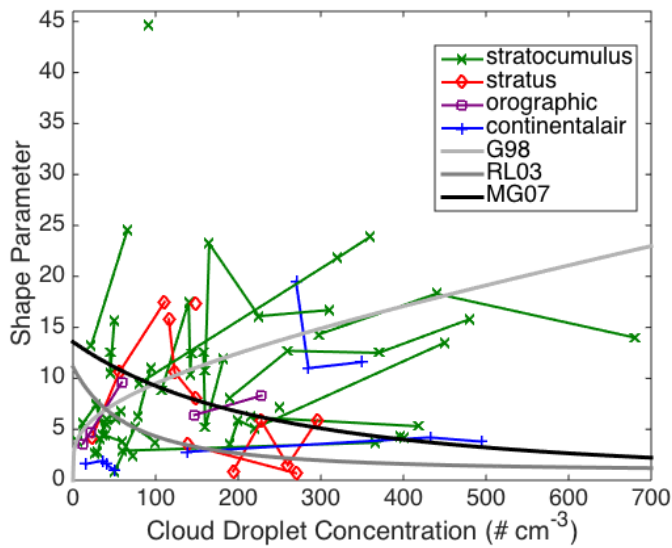
747

748

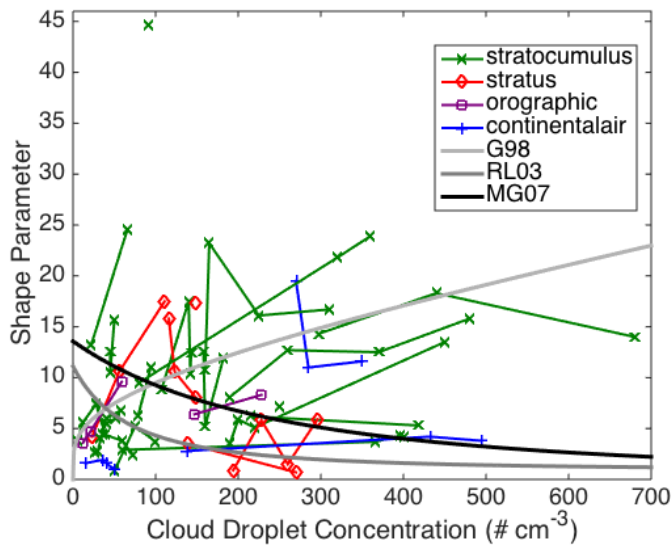


749

750



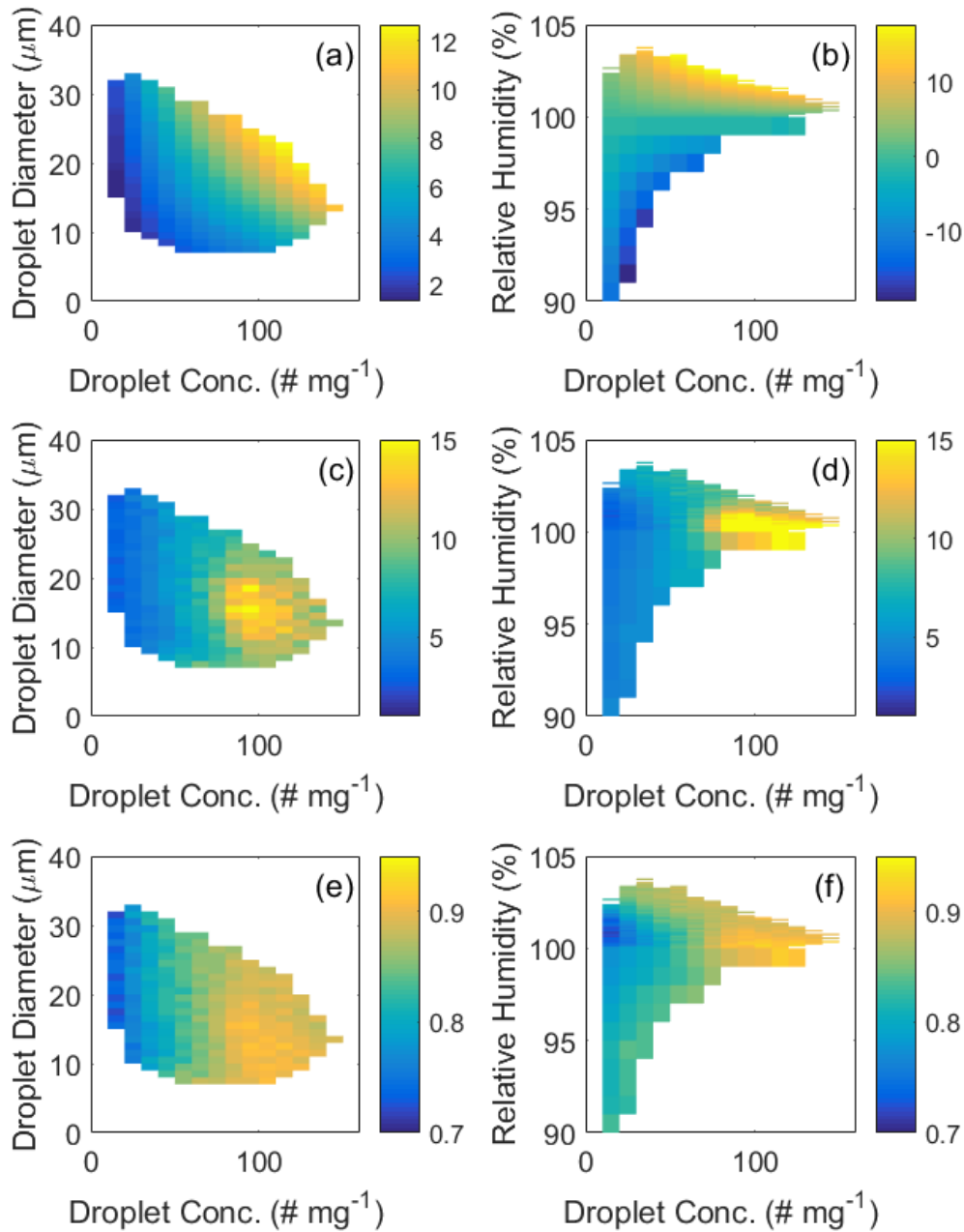
1  
 2 Figure 1. Shape parameter ( $\nu$ ) values as a function of cloud droplet concentration as



3 reported by Miles et al. (2000) using  
 4 16 previous studies. Values, cloud classification, and groupings are based on their Tables 1  
 5 and 2. The three solid gray lines show proposed relationships between the cloud droplet  
 6 concentration and the shape parameter. G98 is from Eq. 9 in Grabowski (1998). RL03 is  
 7 from Eq. 3 in Rotstajn and Liu (2003) with their  $\alpha=0.003$ . MG07 is from Eq. 2 in Morrison  
 8 and Grabowski (2007). All equations were originally written for relative dispersion, which  
 9 is equal to  $\nu^{-1/2}$ , and have been converted to equations for  $\nu$  for this figure.

10

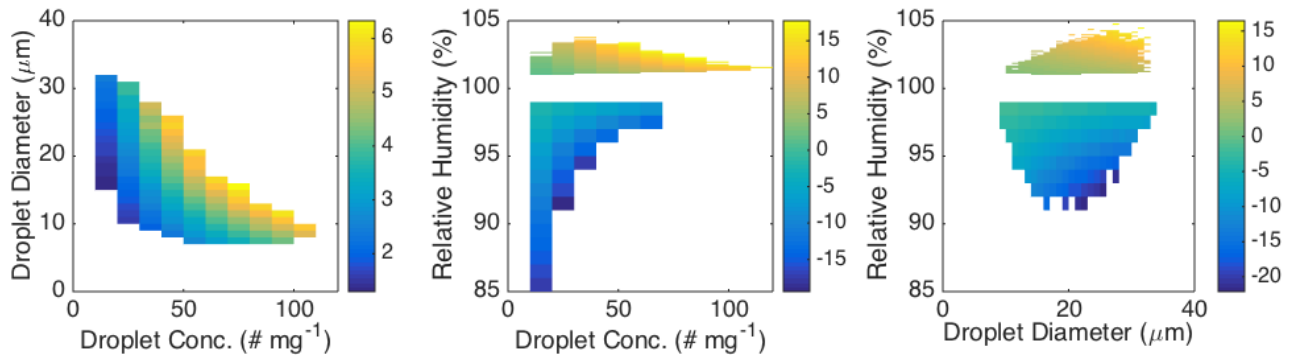
11



12

13 Figure 2. (a, b) Example average condensation and evaporation rates ( $\text{mg kg}^{-1} \text{s}^{-1}$ ), (c, d)  
 14 example average shape parameters, and (e, f) example average values of  $\overline{f_{NU, BIN}}$  in joint  
 15 bins from BIN400. (a, c, e) show average values of the two quantities for all joint bins from  
 16 BIN400 with  $S$  between 1.011-1.012 and (b, d, f) show averages for all joint bins from

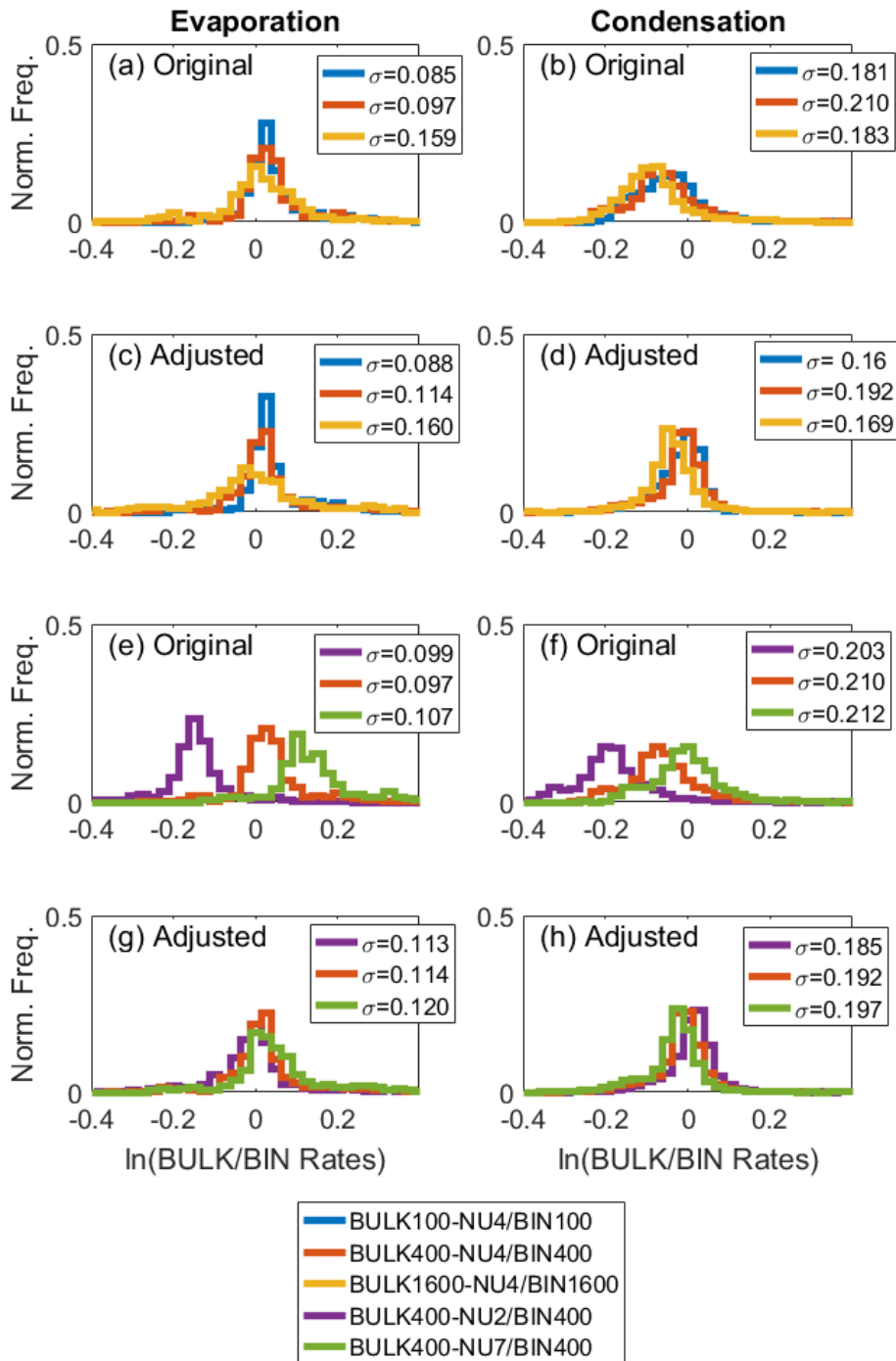
17 BIN400 with  $\bar{D}$  between 19 and 20 $\mu\text{m}$ .



18

19 Figure 2. The average condensation and evaporation rates ( $\text{g kg}^{-1} \text{s}^{-1}$ ) in joint bins from  
20 BIN400. (a) Joint bins where the relative humidity is 101-101.1% (b) Joint bins where the  
21 cloud droplet diameter is 18-19  $\mu\text{m}$ . (c) Joint bins where the cloud droplet concentration is  
22 20-21  $\text{mg}^{-1}$ . See the text for more information about the joint bins.

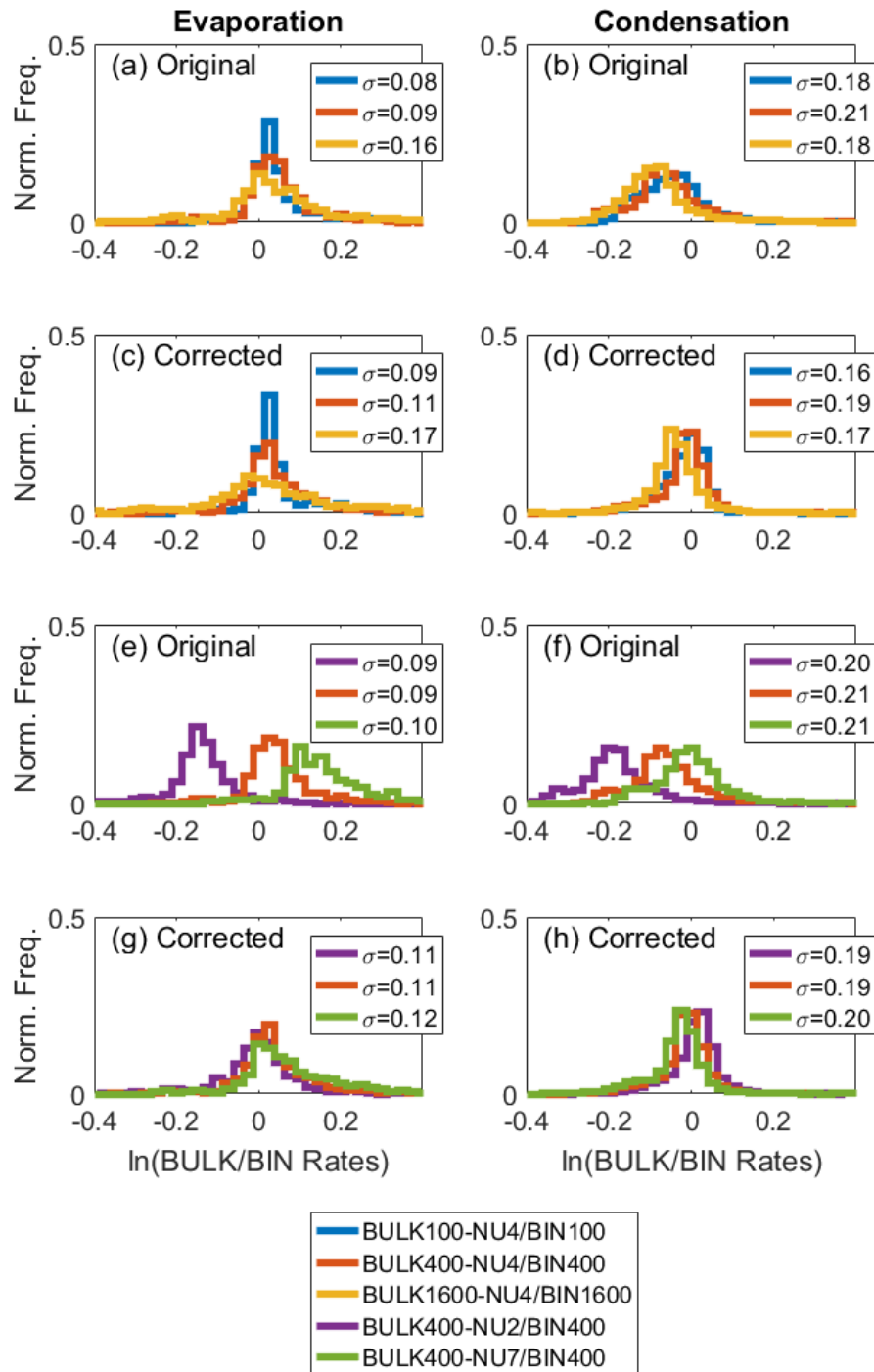
23



24

25 Figure 3. The ratio of the BULK to BIN (a-c) condensation and (d-f) evaporation rates as a  
 26 function of saturation ratio ( $S$ ) and integrated diameter ( $N\bar{D}$ ) for each pair of simulations.

27 Note the differences in axes limits.

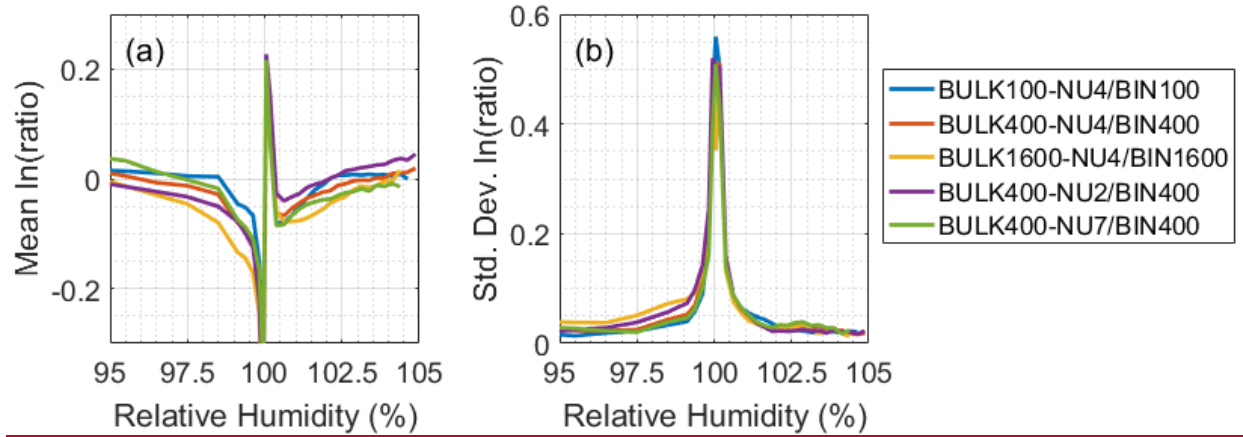


28

29 Figure 3. Normalized histograms showing the logarithm of the ratio of BULK to BIN (a, c, e,

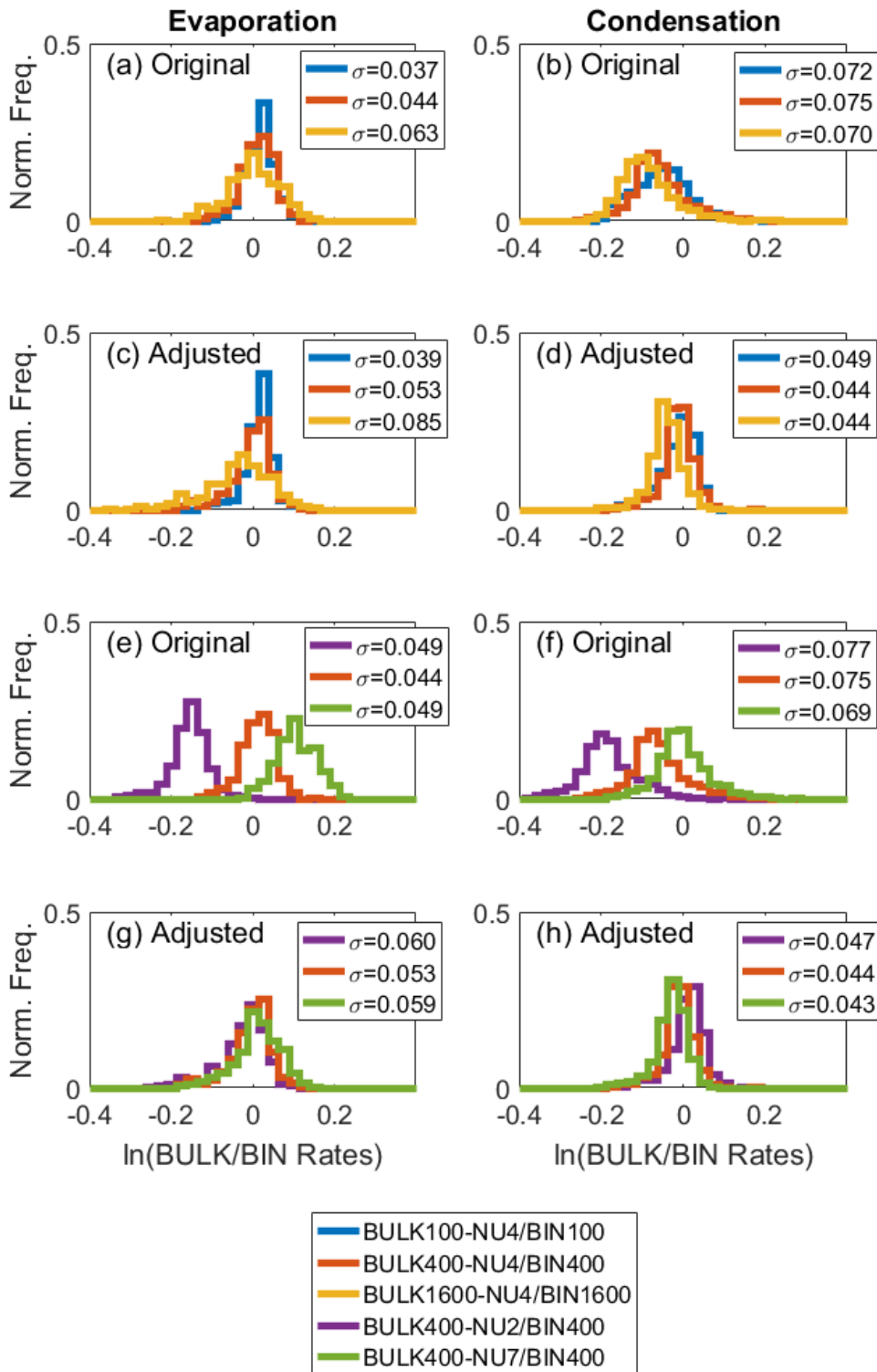
30 g) evaporation and (b, d, f, h) condensation rates. (a-b) and (e-f) show histograms using the

31 original data, and (c-d) and (g-h) show histograms where the correction in Eq. (4) has been  
32 applied.



33  
34  
35  
36

Figure 4. The (a) mean ln(ratio) and (b) standard deviation of the ln(ratios) as a function of relative humidity for all five simulation pairs.

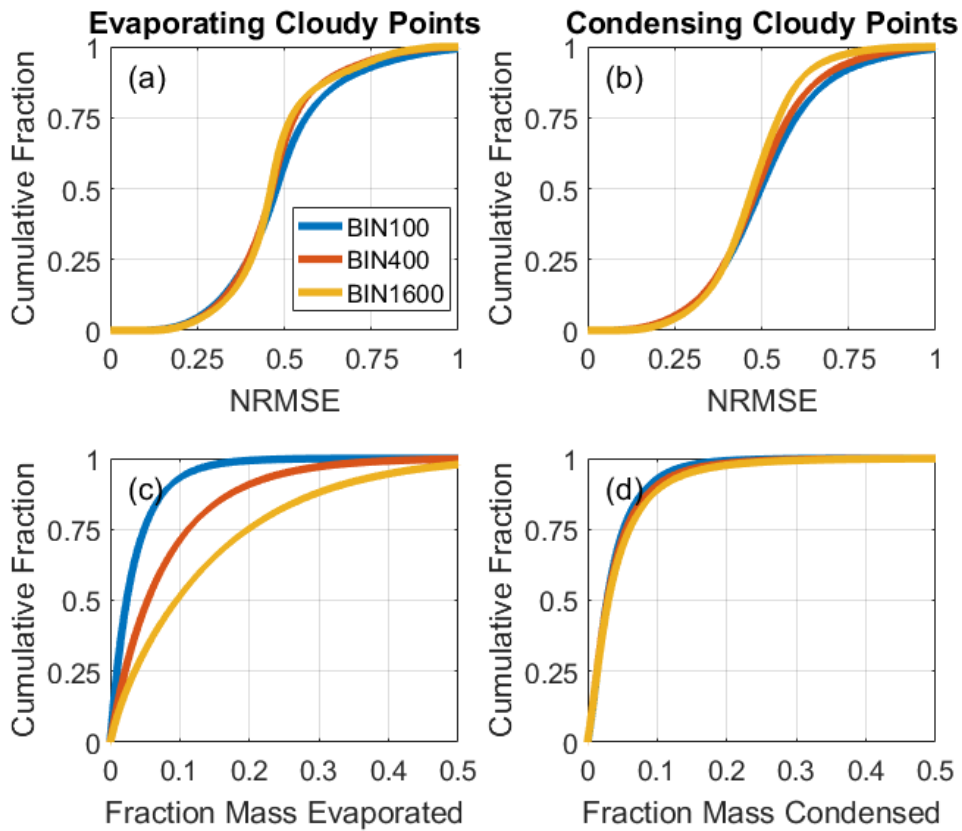


37

38 Figure 5. Like Figure 3, but excluding grid points from the joint bins with relative humidity

39 between 99.5% and 100.5%.

40  
41

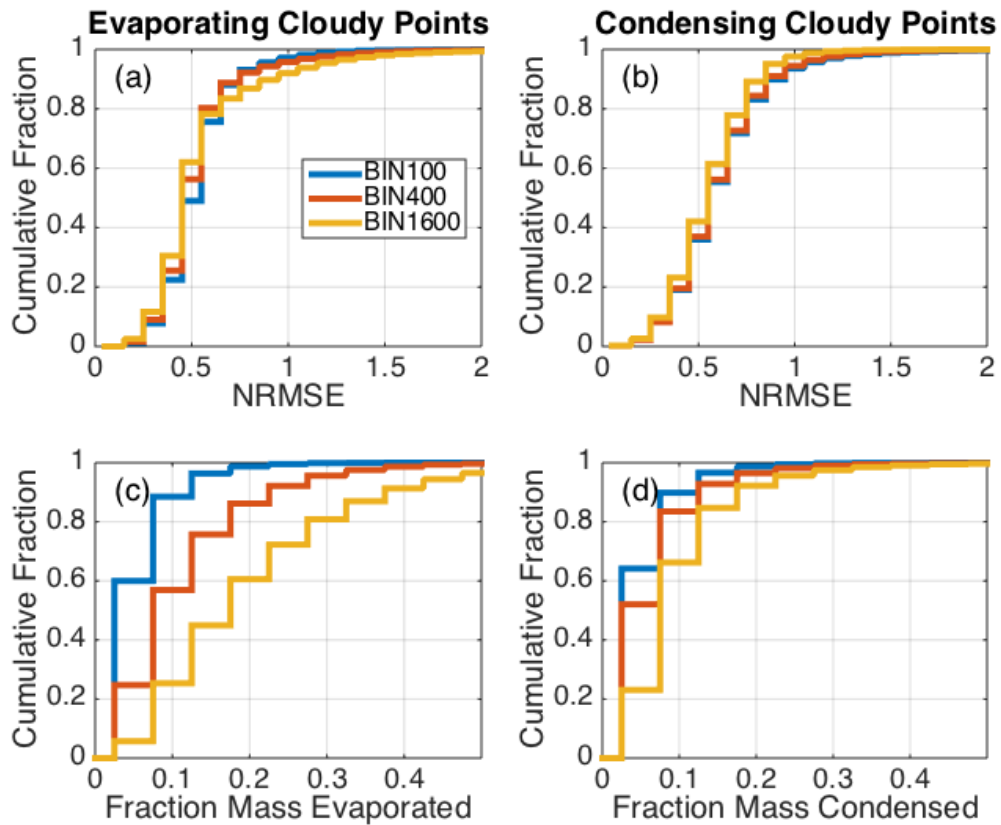


42  
43

---

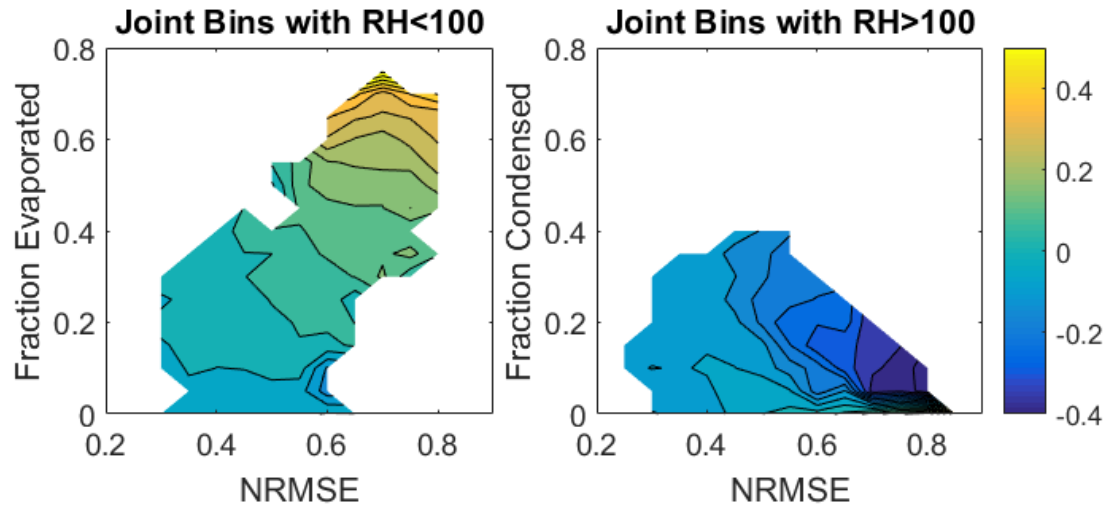
44 Figure 6. Cumulative distributions of (a, b) NRMSE, (c) fraction of mass evaporated, and (d)  
45 fraction of mass condensed. (a, c) include only grid points where evaporation occurred and  
46 (b, d) include only grid points where condensation occurred.

47



49

50 **Figure 4. Cumulative histograms of (a-b) the normalized root mean square error (NRMSE)**  
 51 **of the fitted gamma PDFs to the simulated cloud droplet size distributions in all three BIN**  
 52 **simulations and (c-d) the fraction of cloud mass evaporated or condensed in a time step in**  
 53 **all three BIN simulations. (a, c) show evaporating cloudy points and (b, d) show condensing**  
 54 **cloudy points.**

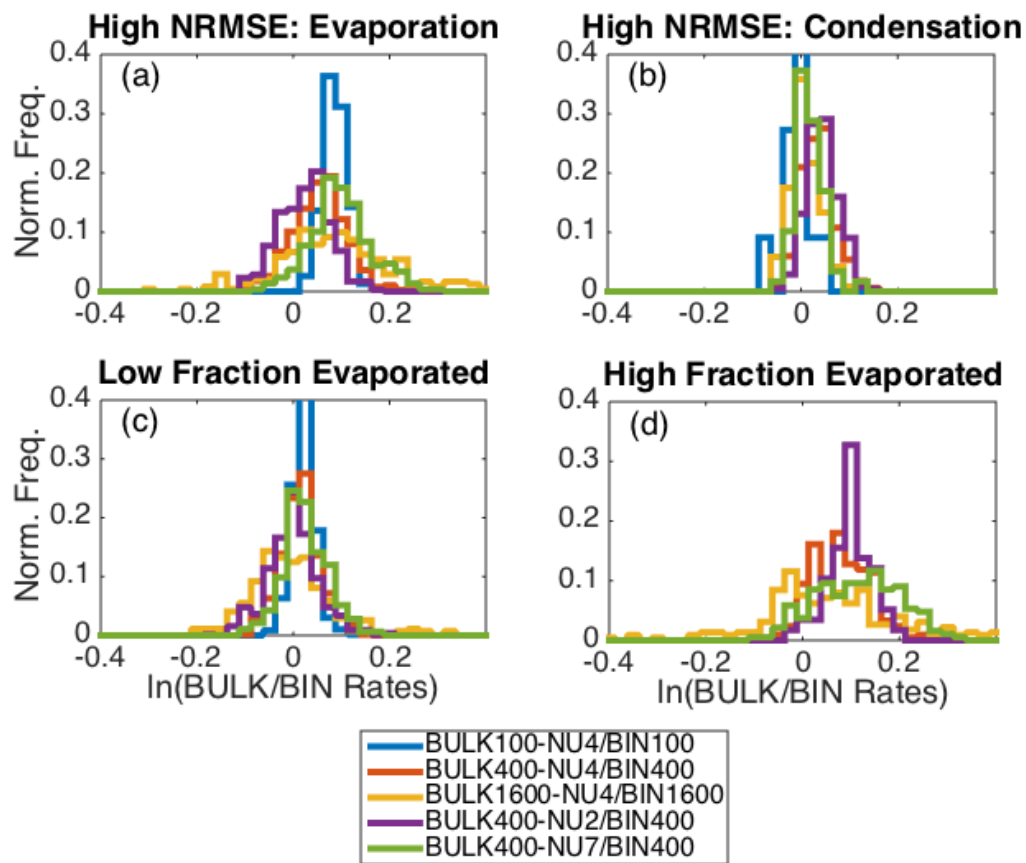


55

---

56 Figure 7. For each joint  $S$ ,  $N_t$ , and  $\bar{D}$  bin, the mean NRMSE and mean fraction of mass  
 57 evaporated or condensed was calculated. Each panel shows the relationship between the  
 58 mean NRMSE, mean adjusted  $\ln(\text{ratio})$  (colors), and (a) mean fraction of mass evaporated  
 59 or (b) mean fraction of mass condensed. Joint bins from all simulation pairs are included in

60 the mean adjusted  $\ln(\text{ratios})$  that are shown.



61

62 Figure 5. Similar to Figure 3. Histograms of the logarithm of the ratio of BULK to BIN  
63 condensation and evaporation rates but with conditional sampling of the data. (a-b) Only  
64 BIN simulation data points with an NRMSE greater than 0.6 are included in the analysis. (a)  
65 Shows evaporation and (b) shows condensation. (c) Only BIN and BULK simulation data  
66 points where the fraction of evaporated mass in one time step is less than 0.25 and (d)  
67 where the fraction of evaporated mass is greater than 0.25 are included in the analysis.

68